

Article

A Convenient One-Pot Synthesis of a Sterically Demanding Aniline from Aryllithium Using Trimethylsilyl Azide, Conversion to β -Diketimines and Synthesis of a β -Diketimate Magnesium Hydride Complex

 Nikita Demidov , Mateus Grebogi, Connor Bourne, Aidan P. McKay, David B. Cordes  and Andreas Stasch * 

EaStCHEM School of Chemistry, University of St Andrews, North Haugh, St Andrews KY16 9ST, UK; nd49@st-andrews.ac.uk (N.D.); mateus0303@icloud.com (M.G.); cb376@st-andrews.ac.uk (C.B.); apm31@st-andrews.ac.uk (A.P.M.); dbc21@st-andrews.ac.uk (D.B.C.)

* Correspondence: as411@st-andrews.ac.uk; Tel.: +44-(0)-1334-463-382

Abstract: This work reports the one-pot synthesis of sterically demanding aniline derivatives from aryllithium species utilising trimethylsilyl azide to introduce amine functionalities and conversions to new examples of a common N,N' -chelating ligand system. The reaction of TripLi ($\text{Trip} = 2,4,6\text{-}i\text{Pr}_3\text{-C}_6\text{H}_2$) with trimethylsilyl azide afforded the silyltriazene $\text{TripN}_2\text{N}(\text{SiMe}_3)_2$ in situ, which readily reacts with methanol under dinitrogen elimination to the aniline TripNH_2 in good yield. The reaction pathways and by-products of the system have been studied. The extension of this reaction to a much more sterically demanding terphenyl system suggested that TerLi ($\text{Ter} = 2,6\text{-Trip}_2\text{-C}_6\text{H}_3$) slowly reacted with trimethylsilyl azide to form a silyl(terphenyl)triazene lithium complex in situ, predominantly underwent nitrogen loss to $\text{TerN}(\text{SiMe}_3)\text{Li}$ in parallel, which afforded $\text{TerN}(\text{SiMe}_3)\text{H}$ after workup, and can be deprotected under acidic conditions to form the aniline TerNH_2 . TripNH_2 was furthermore converted to the sterically demanding β -diketimines $^{\text{RTrip}}\text{nacnacH}$ ($=\text{HC}\{\text{RCN}(\text{Trip})\}_2\text{H}$), with $\text{R} = \text{Me}, \text{Et}$ and $i\text{Pr}$, in one-pot procedures from the corresponding 1,3-diketones. The bulkiest proligand was employed to synthesise the magnesium hydride complex $[\{i\text{Pr}^{\text{Trip}}\text{nacnac}\}\text{MgH}]_2$, which shows a distorted dimeric structure caused by the substituents of the sterically demanding ligand moieties.

Keywords: aniline synthesis; azides; β -diketimates; magnesium hydride; metal-halogen exchange; organolithium reagents; sterically demanding N -ligands; terphenyl ligands; triazenes



Citation: Demidov, N.; Grebogi, M.; Bourne, C.; McKay, A.P.; Cordes, D.B.; Stasch, A. A Convenient One-Pot Synthesis of a Sterically Demanding Aniline from Aryllithium Using Trimethylsilyl Azide, Conversion to β -Diketimines and Synthesis of a β -Diketimate Magnesium Hydride Complex. *Molecules* **2023**, *28*, 7569. <https://doi.org/10.3390/molecules28227569>

Academic Editor: Yves Canac

Received: 19 October 2023

Revised: 8 November 2023

Accepted: 9 November 2023

Published: 13 November 2023



Copyright: © 2023 by the authors. Licensee MDPI, Basel, Switzerland. This article is an open access article distributed under the terms and conditions of the Creative Commons Attribution (CC BY) license (<https://creativecommons.org/licenses/by/4.0/>).

1. Introduction

Sterically demanding N -ligands [1–6] have been driving advances in numerous areas of chemical research. In main group chemistry, for example, the introduction of sterically demanding N -ligands and related species has led to the discovery of compound classes with low coordination numbers in a variety of oxidation states, which stabilised molecular entities in unusual bonding modes that were found to show unique properties and novel reactivities [7–9]. In addition to effects on compound properties and reactivity instilled by the ligand class attached to central elements, steric effects have a strong influence on compound properties, including on coordination numbers and allowing or preventing certain reaction pathways. The interplay of steric demand, including considerations of repulsion from sheer size and ligand shape [10,11], and attractive effects between ligands, substituents, and central elements from London dispersion forces [12–14], paints a more complex picture of the effects bulky ligands have on various compound classes. As such, surprising effects on the chemistry of unusual compound classes stabilised by sterically demanding ligands have often been discovered by exploratory investigation of the sterics and electronics of their ligands. For example, in magnesium β -diketimate chemistry,

which is of relevance here, relatively small changes in ligand sterics have led to significantly different product outcomes for magnesium hydride [15,16] and low oxidation state magnesium [17–19] chemistry.

The introduction of new sterically demanding ligands bearing different substituents to the chemistry of the elements led to novel classes of compounds [7] that, for the bulkiest systems, show coordination numbers down to one. In selected cases, these have displayed unique structures, bonding modes, and reactivities, for example in Al [20], Ge [21], P [22], Sb [23] and Bi [24] species, but the steric bulk can also pose significant new challenges for the syntheses of these new (pro)ligand entities. Due to the increased steric demand in these ligands, common synthetic techniques may prove less applicable to the task, or suitable, convenient starting materials are not readily commercially available. Thus, facile synthetic techniques are required to expand our toolset to access new ligands. Here, we explore the conversion of bulky aryl halides to reactive organolithium compounds, their further transformation to aniline derivatives, the synthesis to a common proligand class, and an example metal complex.

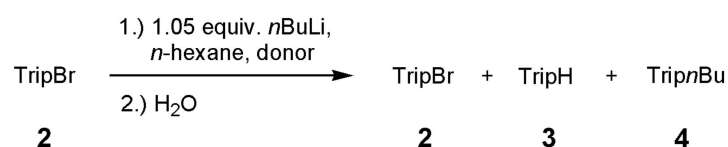
2. Results and Discussion

The aim of the first part of the study was to find a convenient one-pot procedure that would allow the synthesis of substituted anilines [25–28] from aryl lithium compounds with techniques and methods suitable for, and familiar to, the synthetic inorganic and organometallic communities. Many methods for electrophilic amination reactions have been developed [29–34], including some to selectively prepare primary amines, but many also show some drawbacks or limitations, and an important consideration for the work described herein was that it could be applied to highly sterically demanding systems. Other synthetic routes to sterically demanding anilines have been successfully developed, but these require either multi-step protocols and/or high pressure set-ups [35–38] or modify the substituents via palladium-catalysed cross-coupling reactions [39]. For this study we decided on using the 2,4,6-triisopropylphenyl substituent, Trip, due to the commercial availability of starting materials, rarer use of the respective aniline compared with the ubiquitous Dip (2,6-diisopropylphenyl) congener, and the use of isopropyl substituents as suitable groups for ^1H NMR spectroscopic investigations.

2.1. Lithiation of TripBr

In order to devise a convenient aniline synthesis via an organometallic route, the first consideration was to revisit the generation of TripLi **1** from commercially available TripBr **2**. Some crystallographically characterised TripLi species [40,41] are known, and are prepared using metal-halogen exchange [42,43], with *n*-butyllithium as the lithiating agent. The metal-halogen exchange reaction is an equilibrium system [44] that forms a stabilised mixture, and the thermodynamics and kinetics are influenced by solvent effects [45–47], and the steric and electronic nature of the substituents [48,49]. Furthermore, side reactions such as C–C coupling [50] and ether cleavage [51] can lead to consumption of lithium reagent and substrate, potentially hampering efficient conversion to the desired product. In addition, we envisaged that further conversions of in situ generated aryllithium species for the synthesis of sterically demanding systems might require harsher conditions for onward reactivity. As such, we were interested in a quite robust lithiation protocol that can tolerate non-cryogenic conditions, e.g., room temperature, at least for onward reactivity, and would also work for electron-rich aryl substituents. To briefly test and ensure sufficient in situ lithiation for further conversions, TripBr **2** was treated with 1.05 equivalents of *n*BuLi under varying conditions and the mixture was hydrolysed and the product ratio was analysed by ^1H NMR spectroscopy, see Scheme 1 and Table 1. The relative percentages of the main products TripBr **2**, i.e., unreacted starting material, TripH **3** as a proxy for hydrolysed TripLi **1**, and the coupled product Trip*n*Bu **4** were added to 100% and represent the main products. Traces of TripOH **5**, likely from the reaction of TripLi **1** with trace amounts of air, for example, formed during the quenching process, were also present in some samples.

Inspecting the lithiation results summarised in Table 1, diethyl ether (entry 1) as a donor led to insufficient conversion. Using only one or a half equivalent of the more powerful donor solvent THF per Li centre (entries 2 and 3) afforded poor conversion of TripBr 2. More THF per Li as a donor (2–5 equivalents, entries 4–7) provided good conversion of 2 to 1, by implication, but also saw increasing quantities of Trip*n*Bu 4 formed from direct C–C coupling [50]. The latter issue could be suppressed by cooling the reaction solution to $-20\text{ }^{\circ}\text{C}$ (entry 8), which decreased the coupling to Trip*n*Bu 4 and was beneficial for the lithiation of TripBr 2, possibly due to forming more reactive lower aggregates for entropic reasons [52] and/or less ether cleavage [51]. To test how competitive ether cleavage is under the conditions, the experiment for entry 7 (Table 1) was repeated, but the *n*BuLi was added to the solvent mixture and left for 30 min at room temperature before TripBr 2 was added and reacted for 30 min before hydrolysis and analysis (entry 9). This experiment provided significant unreacted 2 likely because some *n*BuLi degraded via ether cleavage under these conditions. This highlights that ether cleavage is a significant issue even for relatively low THF concentrations and suggests that these issues are remedied at the lower temperature used in the conditions of entry 8. Going forward, the conditions for entry 8 were used in subsequent sections.



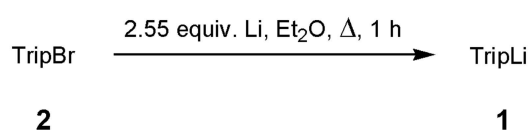
Scheme 1. Lithiation of TripBr 2.

Table 1. Lithiation study of TripBr 2.

Entry	Donor, Equiv. per Li ^a	Temperature, <i>T</i>	TripBr 2	TripH 3 (c.f. TripLi 1)	Trip <i>n</i> Bu 4
1	Et ₂ O, 17:1	r.t.	41.5	58.5	~0
2	THF, 0.5:1	r.t.	92.2	7.8	~0
3	THF, 1:1	r.t.	68.0	32.0	~0
4	THF, 2:1	r.t.	23.2	74.8	2.0
5	THF, 3:1	r.t.	12.9	83.3	3.8
6	THF, 4:1	r.t.	9.8	84.7	5.4
7	THF, 5:1	r.t.	6.6	85.7	7.7
8	THF, 5:1	$-20\text{ }^{\circ}\text{C}$	trace	>97	trace
9	THF, 5:1 (+ <i>n</i> BuLi first) ^b	r.t.	36.1	61.8	2.1

^a 1.05 equivalents of *n*BuLi solution were added dropwise to TripBr in *n*-hexane plus donor solvent as given to afford a 0.395 M reaction solution, stirred for 30 min, then hydrolysed with water and the organic residues were analysed by ¹H NMR spectroscopy (CDCl₃), reporting the percentages of the products 2, 3 and 4 from their relative ratios. The experiments were conducted with the same reagent concentrations as single experiments only to allow for a brief study to find favourable conditions. Estimated error $\pm 1\text{--}2\%$. In addition, trace amount of TripOH, presumably from traces of oxygen were present in some samples. ^b *n*BuLi was first reacted with the solvent mixture for 30 min before TripBr was added and the experiment continued.

An alternative to using *n*BuLi is the direct reaction of TripBr 2 with lithium metal in diethyl ether for one hour under reflux to TripLi 1, see Scheme 2, which is straightforward and afforded a good overall yield after in situ conversion to the desired aniline product, vide infra.

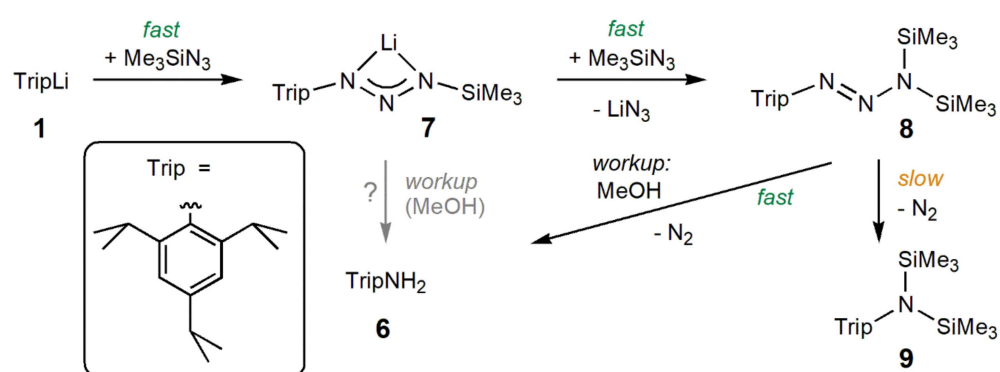


Scheme 2. Lithiation of TripBr 2.

2.2. Reaction of TripLi 1 with TMSN₃

Reactions of organometallic compounds and organic azides [29,53–56] can form triazenes [57], including sterically demanding triazenides [58,59]. In the past, the group of N. Wiberg has studied reactions of s-block organometallics with silylazides and the synthesis and properties of silyltriazenes [60–67]. Subsequently, reactions of specialised organic azides with Grignard or organolithium reagents have been utilised as NH₂⁺ synthons to successfully afford amines or anilines that show various advantages and limitations. Trimethylsilylmethyl azide [68–70] and azidomethyl phenyl sulfide [71–73] have been shown to be effective in reactions with Grignard reagents, which can be challenging to form for electron-rich substrates [74], but these azide systems struggle when reacted with organolithium reagents. Diphenylphosphoryl azide affords satisfactory to good yields with either of these classes of organometallic reagents but is more expensive and requires harsh hydrolysis conditions [75]. Vinyl or allyl azides have shown high efficiency [76,77], but are not commercially available and are likely more hazardous to handle [53]. To introduce an alternative that uses a commercially available and relatively stable azide, we proposed that the reaction between an organolithium species, and by implication other electropositive organometallics, and a silylazide would lead to a silyl(organo)triazenide lithium complex, which could be easily worked up to a primary amine in a one-pot procedure. Nucleophilic attack of an organometallic substituent on the (outer) azide nitrogen atom also seemed like a procedure that could be facile even for highly sterically demanding systems, as suggested by the syntheses of bulky triazenides [58,59] and terphenyl azide compounds [78–80]. Although syntheses for TripNH₂ 6 are known [81–85], most involve the synthesis and reduction of TripNO₂, which has some drawbacks such as expensive and/or hazardous reagents, multi-step protocols, and relies on the accessibility of the nitro derivative.

Initially, the reaction of TripLi 1, prepared according to either Scheme 1 or Scheme 2, with one equivalent of trimethylsilyl azide (azidotrimethylsilane, Me₃SiN₃) at room temperature proceeded rapidly. We found that simple quenching with (wet) methanol provided rapid gas formation, and crude TripNH₂ 6 was obtained after workup—an observation that was in line with our expectation of a pathway via an intermediate silyl(organo)triazenide lithium complex, complex 7 in Scheme 3 (grey arrow). The yield of TripNH₂ 6, however, did not significantly exceed 40%, and large quantities of TripH 3 were obtained alongside 6, independent of reaction times. Furthermore, an insoluble precipitate formed during the reaction. Adding further Me₃SiN₃, however, increased the yield of TripNH₂ 6, and the consistently formed insoluble by-product precipitated from the reaction mixture early on. The latter was identified as LiN₃ via its properties, NMR, and IR spectroscopic studies, and suggests that further silylation of 7 with Me₃SiN₃ occurs, i.e., the azide is acting as a pseudohalide, resulting in the formation of disilyl(organo)triazene TripN₂N(SiMe₃)₂ 8. Evidence for the formation of 8 comes from an NMR spectroscopic study that shows an intermediate with two chemically identical SiMe₃ groups by integration and a ¹⁵N NMR resonance [86,87] detected via a 2D ¹H-¹⁵N HMBC NMR experiment of a silyl-bound nitrogen atom at δ 187 ppm in deuterated benzene. Derivatives of 8, such as PhN₂N(SiMe₃)₂, have been obtained by Wiberg previously, and some of these products decomposed with dinitrogen elimination [64]. Treating 8 with methanol gave rapid gas evolution and afforded TripNH₂ 6. Reactions performed on a larger scale also afforded small and varying quantities of TripN(SiMe₃)₂ 9, which could be structurally characterised (Figure 1), alongside the main product TripNH₂ 6. Compound 9 is typically present in low percentages as a by-product from these reactions, and it is likely that during the synthesis, some TripN₂N(SiMe₃)₂ 8 decomposes and loses dinitrogen to form TripN(SiMe₃)₂ 9 (Scheme 3). In contrast to 8, a ¹⁵N NMR resonance of δ 43 ppm (in CDCl₃, via a 2D ¹H/¹⁵N HMBC NMR experiment) was found for TripN(SiMe₃)₂ 9. As expected, the nitrogen centre in 9 is planar (sum of angles: ca. 360°) in its molecular structure (Figure 1), c.f. the structure of N(SiMe₃)₃ [88], and the metrical features are as expected.



Scheme 3. Reactions of TripLi **1** with Me₃SiN₃.

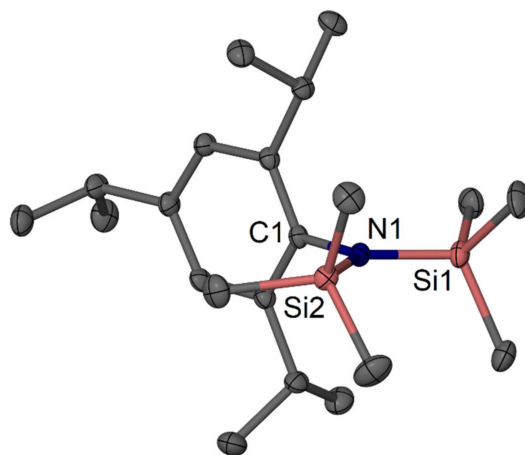


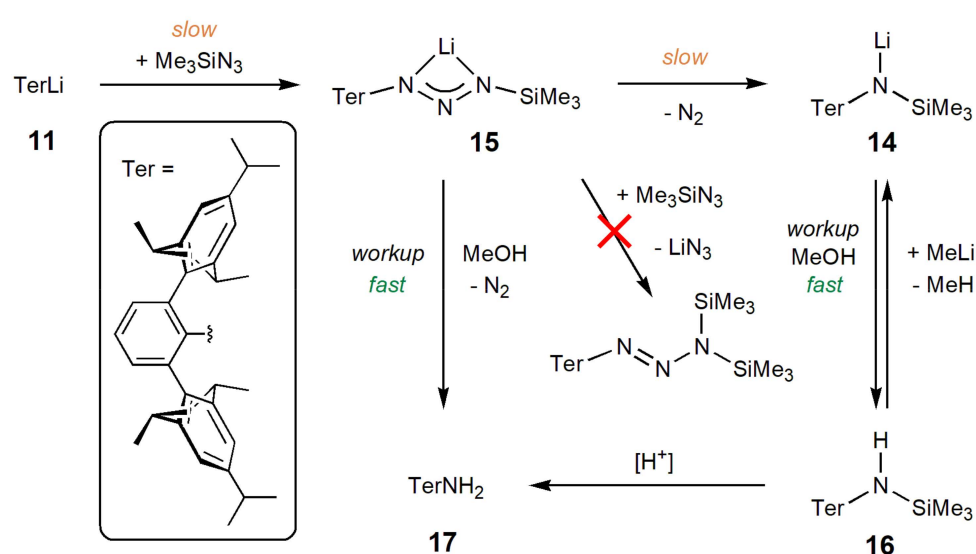
Figure 1. Molecular structure of TripN(SiMe₃)₂ **9**, 30% thermal ellipsoids. Hydrogen atoms omitted. Selected bond lengths (Å) and angles (°): Si1–N1 1.7497(19), Si2–N1 1.7554(19), N1–C1 1.450(3); Si1–N1–Si2 123.82(10), C1–N1–Si1 120.42(14), C1–N1–Si2 115.75(14).

A simple aqueous workup of the reaction mixtures afforded crude TripNH₂ **6** in good, isolated yields. The crude product can be dried under vacuum, removing some volatile by-products, which would include small molecules from ether cleavage and could include smaller amines (e.g., *n*BuNH₂, b.p. ca. 78 °C) from side reactions. This leaves predominantly TripNH₂ **6** as the main product, but also the possible high-boiling by-products TripBr **2** from insufficient lithiation, TripH **3** from protonolysis, Trip*n*Bu **4** from C–C coupling, TripOH **5** from oxidation and TripN(SiMe₃)₂ **9** from loss of dinitrogen of the intermediate **8**. Gratifyingly, none of the Trip-containing by-products readily reacted with acids and the crude product could be treated with aqueous HCl and petroleum ether or hexane as a two-phase system to afford solid TripNH₃⁺Cl[−] **10** (as a hydrate) for purification that could be further washed with petroleum ether or hexane. Treatment with bases regenerated purer TripNH₂ **6**. Isolated yields of TripNH₂ **6** after this purification from TripBr were 86% (typically ca. 75–86%) via the *n*BuLi route, and 81% via the Li metal route. In addition, the compound can also be purified by column chromatography on alumina with petroleum ether/dichloromethane.

2.3. Extension to a Sterically Demanding Terphenyl System

To study if the above method can be conveniently transferred to another, more sterically demanding ligand system, we investigated the terphenyl substituent 2,6-bis(2,4,6-triisopropylphenyl)phenyl, Ter, in this reaction [78,80,89]. Initially, TerLi(OEt)₂ **11**(OEt)₂ was prepared from TerI **12** and *n*BuLi [89] to study its reaction with Me₃SiN₃ on a small scale by NMR spectroscopy. These experiments showed that the reaction is very slow and that significant quantities of TerH **13** are formed alongside some *N*-containing main product, later identified as a TerN(SiMe₃)Li **14** derivative. A significant change in the reaction

kinetics is not surprising when the steric demand of the system is changed dramatically. It is proposed that the hydrogen on TerH **13** originated from Me_3SiN_3 during the reaction and a brief study was undertaken to test the influence of donor solvent addition. When $\text{TerLi}(\text{OEt}_2)$ **11**(OEt_2) was reacted with Me_3SiN_3 in deuterated benzene, after four days at room temperature a ratio of TerH **13** to $\text{TerN}(\text{SiMe}_3)\text{Li}$ **14** of approximately 2:1 was obtained. A reaction with additional five equivalents of the donor solvent diethyl ether under the same conditions was slower (18 days) and the main product ratio changed to approximately 2:3 (**13**:**14**). Changing the donor solvent to THF (5 equivalents) provided an approximate ratio of 1:4 after 7 days at room temperature and 8 h at 60 °C, showing that $\text{TerN}(\text{SiMe}_3)\text{Li}$ **14** can be afforded as the dominant product (also see Table S1). Other observations that were made showed that, in contrast to the reaction with TripLi **1**, only one equivalent of Me_3SiN_3 was required in this bulkier system, and that before **14** forms, the main intermediate, presumed to be $\text{TerN}_2\text{N}(\text{SiMe}_3)\text{Li}$ **15**, the Ter-equivalent of compound **7** (Scheme 3), was produced, see Scheme 4. Due to the very slow formation of $\text{TerN}_2\text{N}(\text{SiMe}_3)\text{Li}$ **15** from the starting materials, nitrogen loss from **15**, yielding $\text{TerN}(\text{SiMe}_3)\text{Li}$ **14**, becomes competitive in parallel. Workup with (wet) methanol afforded $\text{TerN}(\text{SiMe}_3)\text{H}$ **16** from $\text{TerN}(\text{SiMe}_3)\text{Li}$ **14**, whereas reaction mixtures with incomplete conversion and larger quantities of the intermediate $\text{TerN}_2\text{N}(\text{SiMe}_3)\text{Li}$ **15** afforded TerNH_2 **17** after workup, see Scheme 4 for a summary of these pathways. Some evidence for this was obtained by 2D ^1H - ^{15}N HMBC NMR experiments in deuterated benzene where the ^{15}N NMR signal of the Me_3Si -bound nitrogen centre could be measured and compared. These were found at δ 317 ppm for the intermediate $\text{TerN}_2\text{N}(\text{SiMe}_3)\text{Li}$ **15**, δ 115 ppm for $\text{TerN}(\text{SiMe}_3)\text{Li}$ **14** and δ 67 ppm for $\text{TerN}(\text{SiMe}_3)\text{H}$ **16** [76,77]. Furthermore, the reaction of $\text{TerN}(\text{SiMe}_3)\text{Li}$ **14** to $\text{TerN}(\text{SiMe}_3)\text{H}$ **16** was found to be reversible; treatment of **14** with an excess of methanol in an NMR tube afforded **16**, and this mixture could then be treated with an excess of solid MeLi to afford **14** again. So far, we found no evidence for further reaction of $\text{TerN}_2\text{N}(\text{SiMe}_3)\text{Li}$ **15**, with Me_3SiN_3 to $\text{TerN}_2\text{N}(\text{SiMe}_3)_2$ and LiN_3 (Scheme 4), as was analogously observed for the Trip system (Scheme 3). The molecular structures of $\text{TerN}(\text{SiMe}_3)\text{H}$ **16**, shown in Figure 2, and the solvate $\text{TerN}(\text{SiMe}_3)\text{H}\cdot\text{C}_6\text{H}_6$ **16}\cdot\text{C}_6\text{H}_6, were determined and highlight the steric demand around the N atom with a C–N–Si angle of ca. 130°. The molecular structure infers that in solution, the silyl methyl groups of **16** can reside above the flanking Trip -aryls which is likely the reason for the upfield-shifted resonance for the protons of the SiMe_3 group (δ –0.34 ppm).**



Scheme 4. Reactions of TerLi **11** with Me_3SiN_3 at room temperature.

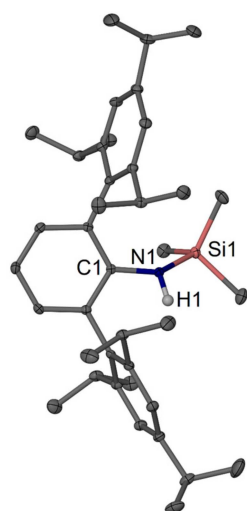
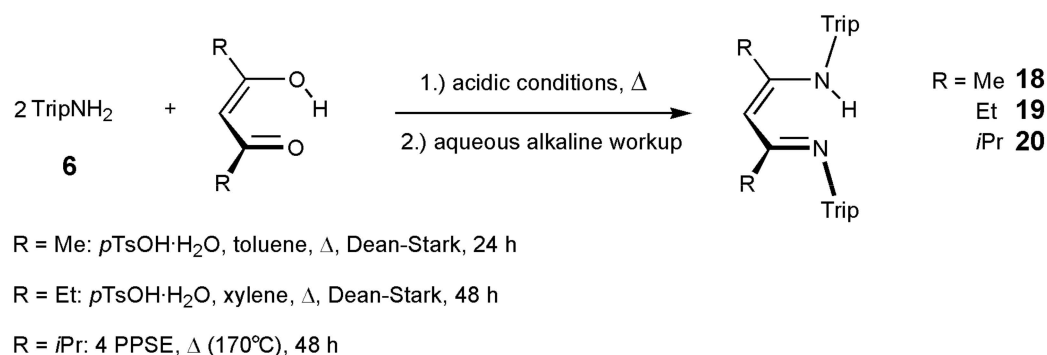


Figure 2. Molecular structure of TerN(SiMe₃)H **16**, 30% thermal ellipsoids. Only the NH hydrogen atom is shown. Selected bond lengths (Å) and angles (°) for **16**: Si1–N1 1.7439(10), N1–C1 1.4080(14); C1–N1–Si1 129.12(7); metrical data for TerN(SiMe₃)H·C₆H₆, **16**·C₆H₆: Si1–N1 1.7423(12), N1–C1 1.4061(17); C1–N1–Si1 133.11(10).

On a preparative scale, TerI **12** was converted with *n*BuLi in an *n*-hexane and diethyl ether mixture to crude TerLi(OEt₂) **11**(OEt₂) and then reacted in situ with Me₃SiN₃ in toluene and 10 equivalents of THF at 60 °C for 20 h, followed by workup with (wet) methanol at 0 °C to afford TerN(SiMe₃)H **16** in 60% isolated yield after recrystallisation from diethyl ether. TerN(SiMe₃)H **16** has been found to desilylate to TerNH₂ **17** when treated with aqueous HCl, or slowly in wet chloroform or with silica gel.

2.4. Synthesis of ^RTripnacnacH Compounds

With the aniline TripNH₂ **6** in hand, we studied its conversion to β-diketimine proligands [2] to progress towards β-diketiminate complexes. The three β-diketimines ^RTripnacnacH, =HC{RCN(Trip)}₂H, with R = Me (**18**), Et (**19**), and *i*Pr (**20**), were prepared by one-pot condensation reactions between TripNH₂ **6** and appropriate 1,3-diketones under acidic conditions, followed by aqueous workup steps under basic conditions, see Scheme 5. Previously, the ^tBuTripnacnacH ligand [83] was prepared via a multi-step route, and a selection of other sterically demanding ^{Me}ArnacnacH proligands, where Ar represents a robust substituent larger than Dip, have been reported in recent years [90–97].



Scheme 5. Synthesis of ^RTripnacnacH compounds **18–20**.

The synthesis of ^{Me}TripnacnacH **18**, generally followed an established protocol [98] and afforded an isolated yield of 76%. β-Diketimines with an ethyl backbone, ^{Et}TripnacnacH **19** (66% yield), are not common, and we have modified an established procedure [98] used for related ligands. The route to the isopropyl backbone-substituted ^{*i*Pr}TripnacnacH **20** (67%

yield) uses a protocol we have recently introduced preparing the related $i\text{PrDip}_{\text{nacnacH}}$ [99], employing the powerful acidic dehydrating agent polyphosphoric acid trimethylsilylester, PPSE [100,101].

The three proligands **18–20** were structurally characterised, see Figure 3, and show the expected overall structure for this ligand class. The molecular structures of **18** and **19** each crystallised with a full molecule in the asymmetric unit and show some preference for alternating long and short N–C/C–C bonds in the ligand backbone, and, accordingly, some localisation of the NH hydrogen atom.

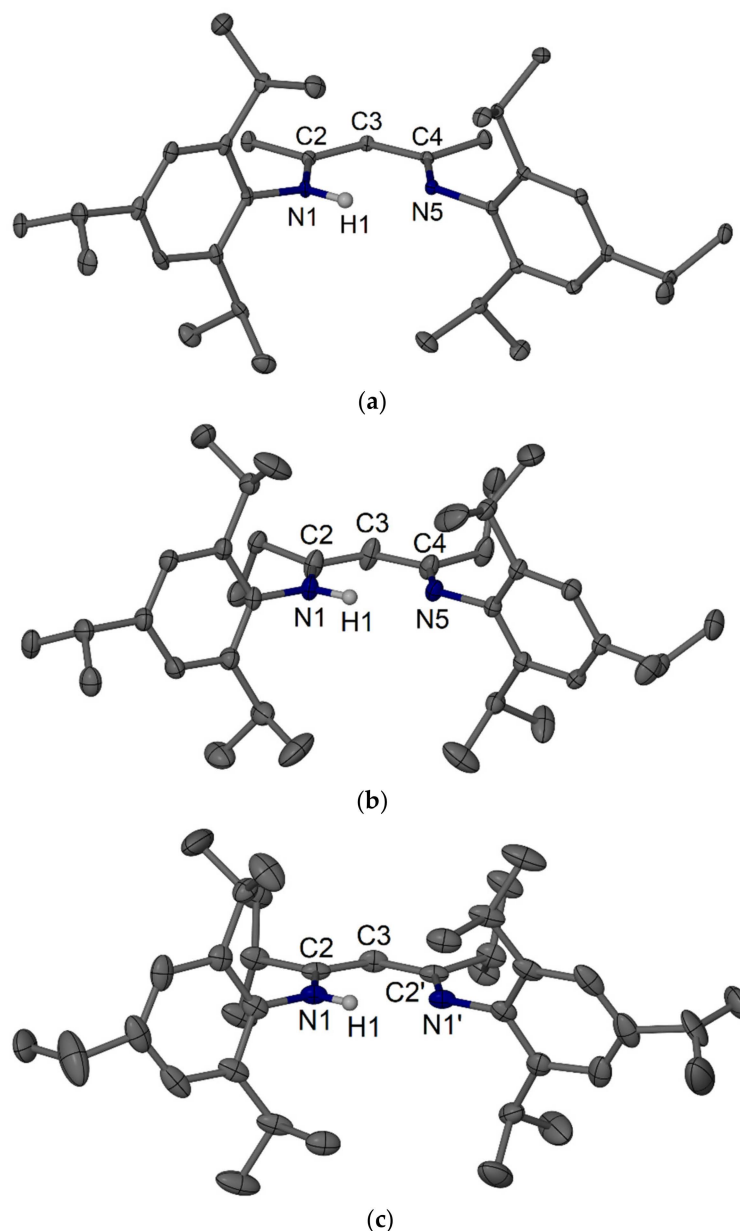
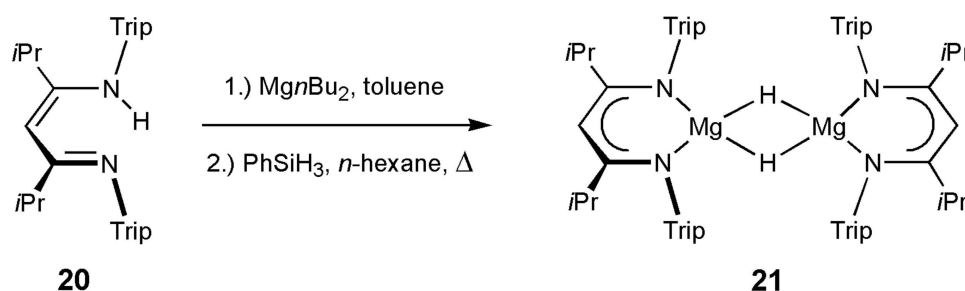


Figure 3. Molecular structures of $\text{MeTrip}_{\text{nacnacH}} \cdot \text{C}_7\text{H}_8$ **18**· C_7H_8 (a), $\text{EtTrip}_{\text{nacnacH}}$ **19** (b) and $i\text{PrTrip}_{\text{nacnacH}}$ **20** (c), 30% thermal ellipsoids. The toluene molecule in **18**· C_7H_8 is omitted. Only NH nitrogen atoms are shown including only one NH position for **20**. Selected bond lengths (Å) and angles (°): **18**· C_7H_8 : N1–C2 1.341(3), C2–C3 1.383(3), C3–C4 1.424(3), N5–C4 1.315(3); C2–N1–C6 123.8(2), C4–N5–C23 121.0(2), N1–C2–C3 121.3(2), C2–C3–C4 125.4(2), N5–C4–C3 121.0(2); **19**: N1–C2 1.346(3), C2–C3 1.372(3), C4–C3 1.428(3), N5–C4 1.305(3); C2–N1–C6 124.87(18), C4–N5–C25 121.83(17), N1–C2–C3 121.5(2), C2–C3–C4 126.8(2), N5–C4–C3 120.06(19); **20**: N1–C2–1.338(3), C2–C3–1.392(3); N1–C2–C3 121.0(2), C2–N1–C4 122.7(2), C2–C3–C2' 127.2(3).

2.5. Synthesis and Characterization of $[(iPr^{Trip}nacnac)MgH]_2$ **21**

To study the impact of the introduction of the Trip substituent to a β -diketiminate system, we used the bulkiest proligand reported herein, $iPr^{Trip}nacnacH$ **20**, to prepare a magnesium hydride complex [16,93,102] for comparison to other related molecules of the type $^{R_{Ar}}nacnacH$ $[(^{R_{Ar}}nacnac)MgH]_2$, where $^{R_{Ar}}nacnac = \{HC\{RCN(Ar)\}$ and R is typically an alkyl group and Ar is a sterically demanding aryl substituent. Using an established protocol [103], $iPr^{Trip}nacnacH$ **20** was treated with $MgnBu_2$ in toluene to form the expected intermediate complex $[(iPr^{Trip}nacnac)MgnBu]$. After removal of all volatiles, the oily residue was taken up in *n*-hexane and reacted for two days at 60 °C with phenyl silane which precipitated clean $[(iPr^{Trip}nacnac)MgH]_2$ **21** in 41% isolated yield (Scheme 6). Complex **21** could be recrystallised from hot benzene to form large colourless crystals that were structurally characterised, see Figure 4. The complex crystallised as a dimeric system, as is found for most other related complexes of the type $[(nacnac)MgH]_2$, with a comparable steric bulk [15,93,103,104], although a few examples of the type $[(nacnac)MgH]$ are known with a monomeric solid state structure with a terminal hydride species and three-coordinate Mg centre [18,91]. The least-square-planes of the two essentially planar β -diketiminate magnesium chelate rings are rotated by approximately 47.6° relative to each other which must be due to the to the alternating “interlocking” contact of the isopropyl groups of the two ligand units which is visualised in the space-filling model in Figure 5, showing the hydrocarbonyl units of both β -diketiminate in different colours. For comparison, β -diketiminate magnesium chelate rings are approximately co-planar in $[(^{MeDip}nacnac)MgH]_2$ [103], approximately orthogonal to each other in $[(^{tBuDip}nacnac)MgH]_2$ [104] but show a similar rotation in $[(^{MeDIPeP}nacnac)MgH]_2$ (DIPeP = 2,6-di(3-pentyl)phenyl) with ca. 42° [93] between metal-ligand planes to accommodate the various bulky substituents on the ligands. An analysis of the buried volume [11] for the Mg centre in **21** ($V_{buried} = 53.5\%$) provided a similar value compared to those for known structurally characterised $[(^{RDip}nacnac)MgH]_2$ complexes ($V_{buried} = 51.1\text{--}56.3\%$), but hints at a more even distribution of the bulk around the metal centre when compared to those of $[(^{RDip}nacnac)MgH]_2$ as judged from inspection the distribution in the four quadrants (see Table S2 in the Supporting Information).



Scheme 6. Synthesis of $[(iPr^{Trip}nacnac)MgH]_2$ **21**.

In solution, $[(iPr^{Trip}nacnac)MgH]_2$ **21** shows 1H NMR resonances for a symmetric compound with a sharp singlet at δ 3.96 ppm for the magnesium hydride resonance in the expected region. The room temperature 1H NMR spectrum shows one broad and two sharp septets, and one broad and three sharp doublets for the isopropyl hydrogen atoms. The broad septet and one broad doublet resonance are associated with one ortho isopropyl group including one methyl group that likely experiences the steric influence from the dimeric interlocked “geometry.” The broad plus one sharp doublet merge above 60 °C and at 80 °C, three resolved septets and three doublets are observed.

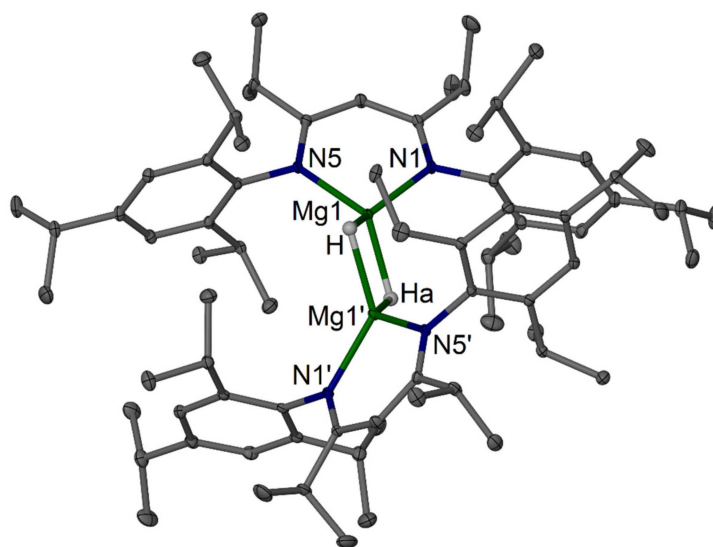


Figure 4. Molecular structures of $[[(\text{iPr}^{\text{Trip}}\text{nacnac})\text{MgH}]_2]$ **21**, 30% thermal ellipsoids. Only MgH hydrogen atoms are shown. Selected bond lengths (Å) and angles (°): Mg1–N1 2.0796(12), Mg1–N5 2.0829(12), Mg1–H 2.029(13), Mg1'–H 2.029(13), Mg1–HA 1.979(14), Mg1⋯Mg1' 2.9502(9), N1–C2 1.3341(18), C2–C3 1.3981(19), C3–C4 1.3987(19), N5–C4 1.3338(18); N1–Mg1–N5 94.40(5), C2–N1–C6 116.64, C4–N5–C27 116.73(11), N1–C2–C3 124.64(13), N5–C4–C3 124.40(13), C2–C3–C4 132.32(14).

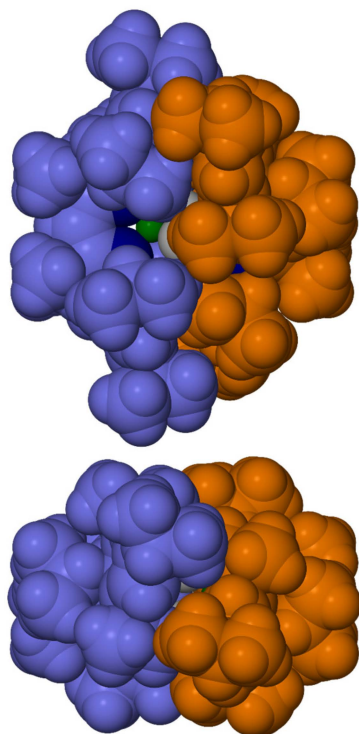


Figure 5. Space-filling model (two views) showing some central atoms (Mg green, N blue, H grey) and the hydrocarbyl groups from the two ligand units in two colours (lavender-purple, rusty orange) showing the “interlocking” isopropyl substituents.

3. Conclusions

Sterically demanding aryllithium compounds can be converted with trimethylsilyl azide to triazene-class intermediates in a one-pot reaction, installing a nitrogen atom at the aryl group and forming aniline derivatives. For two different systems, one with a bulky Trip (Scheme 3) substituent, and one with an extremely bulky terphenyl substituent

(Scheme 4) slightly different (long-lived) intermediates were observed, but the general reactivity is comparable but also influenced by the reaction kinetics resulting from the steric demand of the substituents. An aryllithium can react with trimethylsilyl azide to form silyl(aryl)triazenide lithium, which, for R = Trip, reacted with further trimethylsilyl azide and converted to $\text{TripN}_2\text{N}(\text{SiMe}_3)_2$ **8**. Upon workup with methanol and resulting in dinitrogen formation, this afforded the aniline TripNH_2 **6** in good yield. For the bulkier terphenyl system, the in situ generated silyl(aryl)triazenide lithium species did not react with further trimethylsilyl azide. Instead, this lithiated species formed only slowly enough that it (slowly) lost dinitrogen in parallel and predominantly formed $\text{TerN}(\text{SiMe}_3)\text{H}$ **16** in a one-pot synthesis after treatment with methanol. This silylated aniline derivative is a promising sterically demanding amide proligand in its own right but can also be readily desilylated with acids to afford TerNH_2 **17**. This work shows the main types of intermediates for two systems with highly different steric demands, and gives practical considerations around their synthesis, optimisation, and workup, with the view that the protocol can be easily extended to other substituents and organometallic species for the synthesis of anilines, primary amines, and silylated derivatives. This includes optimised conditions for metal-halogen exchange with *n*-butyllithium that suppress side reactions but allow conversions at relatively high temperatures. Furthermore, TripNH_2 **6** has been further converted in acid-promoted one-pot condensation reactions to the sterically demanding proligands $^{\text{MeTrip}}\text{nacnacH}$ **18**, $^{\text{EtTrip}}\text{nacnacH}$ **19**, and $^{\text{iPrTrip}}\text{nacnacH}$ **20**, the latter of which was converted to the magnesium hydride complex $[(^{\text{iPrTrip}}\text{nacnac})\text{MgH}]_2$ **21**. The significant effects of the steric influence and dispersion forces of the 16 isopropyl groups in **21** will likely impact compound properties and future reactivity.

4. Materials and Methods

4.1. Experimental Details

All manipulations were carried out using standard Schlenk and glove box techniques under an atmosphere of high purity argon or dinitrogen. Tetrahydrofuran, diethyl ether, toluene and *n*-hexane were either dried and distilled under inert gas over LiAlH_4 or taken from an MBraun solvent purification system and degassed prior to use. ^1H , ^7Li , $^{13}\text{C}\{^1\text{H}\}$ and ^1H - ^{15}N HMBC NMR spectra were recorded on a Bruker AVII 400, Bruker AVIII 500, Bruker AVIII-HD 500 or Bruker AVIII-HD 700 spectrometer (Bruker, Billerica, MA, USA) in deuterated benzene or chloroform and were referenced to the residual ^1H or $^{13}\text{C}\{^1\text{H}\}$ resonances of the solvent used, external LiCl in D_2O , or external liquid NH_3 , respectively. Abbreviations: s = singlet, d = doublet, t = triplet, q = quartet, quint = quintet, sext = sextet, sept = septet, br = broad, m = multiplet, e.g., brs, broad singlet; ad denotes an apparent doublet. The IR spectrum was recorded on a neat solid using a Shimadzu IRAfinity 1S IR spectrometer. Melting points were determined in air and are uncorrected. 1-bromo-2,4,6-triisopropylbenzene (TripBr **2**) was degassed and stored over molecular sieves under inert atmosphere. Trimethylsilyl azide (azidotrimethylsilane) and phenylsilane were degassed and stored under inert atmosphere. TerI **12** and $\text{TerLi}(\text{OEt})_2$ **11**(OEt_2) were prepared according to the literature [89]. All other compounds were used as received from chemical suppliers.

CAUTION! Azides are potentially explosive and highly toxic substances, and all manipulations must be carried out by trained workers. Trimethylsilyl azide is considered relatively stable but must not be mixed with acids or water and certain other substances. The aqueous layer during the workup steps below will, or can, contain lithium azide, should be treated accordingly (e.g., collect as a dilute alkaline aqueous solution), and should not be mixed with other waste. A reaction between ionic azides and halogenated reagents and solvents, such as dichloromethane, must be avoided to prevent the formation of explosive azides. The hazards and risks of procedures are dependent on scale. Use suitable gloves when working with azides. Even though no issues were encountered during the work, the use of a blast shield is strongly suggested [53,105,106].

4.2. Syntheses and Formation of Trip Compounds (1–6, 9, 10)

4.2.1. General Procedure for the Optimisation of the Lithium-Bromide Exchange

A Schlenk flask was charged with TripBr **2** (1-bromo-2,4,6-triisopropylbenzene; 0.50 mL, 1.97 mmol), *n*-hexane and the amount of THF or diethyl ether to afford the desired solvent ratio as shown in Table 1. The amount of solvent used for each reaction was determined by calculating the total amount of donor solvent and *n*-hexane (accounting for hexanes from *n*BuLi solution) needed to make a 0.395 M solution of TripBr **2** with the desired donor solvent to Li centre ratio. For an example involving 5 eq. of THF per Li see Section 4.2.2. The reaction mixture was brought to the required temperature and *n*BuLi (1.30 mL, 1.6 M solution in hexanes, 1.05 eq.) was added dropwise. The reaction mixture was stirred for 30 min and quenched with H₂O (ca. 5 mL). All volatiles were removed in vacuo, dichloromethane (ca. 10 mL) and water (ca. 10 mL) were added, and the organic layer was separated. All volatiles were removed in vacuo affording a crude oil that was analysed with ¹H NMR spectroscopy in CDCl₃. Since TripBr **2**, TripH **3** and Trip*n*Bu **4** (plus an occasional minor quantity of TripOH **5** from O₂ capture) are the only Trip-containing products observed, the conversion was calculated directly from the ratio of their aromatic protons, and their sum was assumed as 100% for a qualitative analysis of the lithiation (Table 1).

4.2.2. Synthesis of TripNH₂ **6**

Method 1: A Schlenk flask was charged with TripBr **2** (4.00 mL, 15.79 mmol), *n*-hexane (22.2 mL) and THF (7 mL, ca. 5 THF per Li). The reaction mixture was cooled to −20 °C using a cold bath and *n*BuLi (10.8 mL, 1.6 M solution in hexanes, 1.09 eq.) was added dropwise over approximately two minutes. The reaction mixture was stirred for 30 min at −20 °C and was then placed into a room temperature water bath. After a period of 1–2 min, Me₃SiN₃ (4.80 mL, 36.5 mmol, 2.31 eq.) was added dropwise and the reaction mixture was stirred for a further 30 min. A white precipitate of LiN₃ was formed during that period. The reaction mixture was placed in an ice-water bath (0 °C), the stopper of the flask was removed under a gentle flow of inert gas, and subsequently, methanol (10 mL) was added slowly over a period of 5 min under vigorous gas evolution. Stirring of the mixture was continued until all gas evolution ceased, after which all volatiles were removed in vacuo and the crude product was redissolved in methanol (10 mL) to ensure complete conversion to aniline **6**. After standing for 10 min, all volatiles were removed in vacuo, and DCM (ca. 30 mL) and water (ca. 30 mL) were added, and organic layer was separated. [Note: Be aware that the aqueous layer contains dissolved LiN₃. Ensure that Me₃SiN₃ has reacted and is largely consumed in the procedure; if unsure, use an alkaline solution for carefully quenching of the reaction mixture to ensure no significant quantities of HN₃, are produced.] Removal of all volatiles in vacuo afforded crude TripNH₂ **6** as a yellow-orange oil which may be sufficiently pure for some applications.

Purification: Various methods of purification could be used (e.g., column chromatography using alumina (90), eluent: petroleum ether (40–60 °C) followed by dichloromethane), however, a batch scale purification method via conversion to an anilinium chloride, TripNH₃⁺Cl[−] **10** was found to work best. Conc. aq. HCl (ca. 37%, 12 mL) and petroleum ether (40–60 °C fraction, 10 mL) were added, which produced an off-white precipitate of TripNH₃⁺Cl[−] **10** as a hydrate. The resulting suspension was stirred for 10 min, after which the solid (powder) was isolated by filtration and washed with petroleum ether (10 mL). [Note: A small and varying quantity of TripN(SiMe₃)₂ **9** was obtained in crystalline form by evaporation of the petroleum ether filtrate.] The TripNH₃⁺Cl[−] **10** hydrate solid was redissolved in dichloromethane (40 mL) and (saturated) aqueous Na₂CO₃ (50 mL) was added, and the resulting mixture was stirred for 30 min. The organic layer was separated, the solvent removed in vacuo, and the product was dried under vacuum and afforded TripNH₂ **6** of sufficient purity. Yield: 2.98 g (86%).

Method 2: A Schlenk flask was charged with lithium granules (280 mg, 0.5% sodium, 4–10 mesh, 40.3 mmol, 2.55 eq.), CBr₄ for activation (ca. 2–3 mg), diethyl ether (ca. 30 mL)

and equipped with a reflux condenser and a nitrogen inlet. A solution of TripBr **2** (4.00 mL, 15.8 mmol) in diethyl ether (ca. 8 mL) was added in portions over 30 min to a stirring suspension of lithium granules which initiated an exothermic reaction. After the addition has been completed, the resulting mixture was refluxed for 60 min, cooled to room temperature, allowed to settle, and filtered. To the filtrate, Me₃SiN₃ (4.80 mL, 36.5 mmol, 2.31 eq.) was added dropwise at room temperature and the reaction mixture was stirred for a further 30 min. Workup with methanol and purification were carried out as described above in *Method 1*. Yield: 2.82 g (81%). ¹H NMR (499.9 MHz, CDCl₃, 298 K) δ = 1.29 (d, J_{HH} = 7.0 Hz, 6H, Ar-*p*-CH(CH₃)₂), 1.33 (d, J_{HH} = 6.9 Hz, 12H, Ar-*o*-CH(CH₃)₂), 2.88 (sept, J_{HH} = 6.9 Hz, 1H, Ar-*p*-CH(CH₃)₂), 2.99 (sept, J_{HH} = 6.8 Hz, 2H, Ar-*o*-CH(CH₃)₂), 3.66 (brs, 2H, NH₂), 6.96 (s, 2H, Ar-*H*).

4.2.3. Data for LiN₃

The compound is formed during the synthesis of TripNH₂ **6** and could be isolated directly from the reaction mixture by filtration. The solid also showed a positive flame test for Br suggesting minor LiBr contamination from the reaction mixture. ⁷Li NMR (155.5 MHz, D₂O, 294 K) δ = -0.10 (s, LiN₃). IR (ATR), ν~/cm⁻¹: 2127 (s).

4.2.4. Data for TripN₂N(SiMe₃)₂ **8**

Solid TripLi **1** was obtained by performing a lithiation of TripBr as described for the synthesis of **6** above, via *Method 2*, and storing the concentrated diethyl ether solution at -40 °C. After isolation and briefly drying under vacuum, the obtained crystalline material showed approximately 45% TripLi by weight (with the rest assumed to be ¹H NMR-silent LiBr as judged by integration against an internal standard). TripLi (ca. 3.3 mg, 15.7 μmol) was dissolved in C₆D₆ (0.5 mL) in a J. Young's NMR tube and Me₃SiN₃ (4.6 μL, 35 μmol, ca. 2.23 eq.) was added at 20 °C. Analysis by ¹H NMR spectroscopy showed immediate consumption of TripLi **1** and formation of **8**. ¹H NMR (700.1 MHz, C₆D₆, 295 K) δ = 0.34 (s, 18H, Si(CH₃)₃), 1.26 (d, J_{HH} = 6.9 Hz, 6H, Ar-*p*-CH(CH₃)₂), 1.28 (d, J_{HH} = 7.0 Hz, 12H, Ar-*o*-CH(CH₃)₂), 2.83 (sept, J_{HH} = 7.0 Hz, 1H, Ar-*p*-CH(CH₃)₂), 3.21 (sept, J_{HH} = 6.9 Hz, 2H, Ar-*o*-CH(CH₃)₂), 7.15 (s, 2H, Ar-*H*). ¹³C{¹H} NMR (176.0 MHz, C₆D₆, 295 K) δ = 2.0 (Si(CH₃)₃), 24.2 (Ar-*o*-CH(CH₃)₂), 24.5 (Ar-*p*-CH(CH₃)₂), 28.3 (Ar-*o*-CH(CH₃)₂), 34.8 (Ar-*p*-CH(CH₃)₂), 121.4 (Ar-C), 140.9 (Ar-C), 145.7 (Ar-C), 146.6 (Ar-C). ¹H-¹⁵N HMBS NMR (700.1/70.9 MHz, C₆D₆, 295 K) δ ≈ 187 (TripN₂N(SiMe₃)₂).

4.2.5. Data for TripN(SiMe₃)₂ **9**

The compound was occasionally isolated during the purification of TripNH₂ **6** as described above, especially when the reaction was carried out on a multigram scale (>30 mmol). It remains unclear what factors favour its formation, as preliminary experiments with altered stoichiometry or prolonged reaction time have shown no clear pattern, although heat appears to favour dinitrogen elimination. The compound sublimes at ca. 50 °C (ca. 0.05 mbar) affording colourless crystals that were suitable for X-ray crystallographic analysis. ¹H NMR (700.1 MHz, CDCl₃, 295 K) δ = 0.06 (s, 18H, Si(CH₃)₃), 1.17 (d, J_{HH} = 6.9 Hz, 12H, Ar-*o*-CH(CH₃)₂), 1.21 (d, J_{HH} = 6.9 Hz, 6H, Ar-*p*-CH(CH₃)₂), 2.82 (sept, J_{HH} = 6.9 Hz, 1H, Ar-*p*-CH(CH₃)₂), 3.41 (sept, J_{HH} = 6.9 Hz, 2H, Ar-*o*-CH(CH₃)₂), 6.84 (s, 2H, Ar-*H*). ¹³C{¹H} NMR (176.0 MHz, CDCl₃, 295 K) δ = 2.7 (Si(CH₃)₃), 24.3 (Ar-*p*-CH(CH₃)₂), 25.3 (Ar-*o*-CH(CH₃)₂), 27.6 (Ar-*o*-CH(CH₃)₂), 33.8 (Ar-*p*-CH(CH₃)₂), 121.4 (Ar-C), 140.5 (Ar-C), 144.1 (Ar-C), 146.2 (Ar-C). ¹H NMR (700.1 MHz, C₆D₆, 295 K) δ = 0.16 (s, 18H, Si(CH₃)₃), 1.22 (d, J_{HH} = 6.9 Hz, 6H, Ar-*p*-CH(CH₃)₂), 1.29 (d, J_{HH} = 6.9 Hz, 12H, Ar-*o*-CH(CH₃)₂), 2.79 (sept, J_{HH} = 6.9 Hz, 1H, Ar-*p*-CH(CH₃)₂), 3.58 (sept, J_{HH} = 6.9 Hz, 2H, Ar-*o*-CH(CH₃)₂), 7.05 (s, 2H, Ar-*H*). ¹H-¹⁵N HMBS NMR (700.1/70.9 MHz, C₆D₆, 295 K) δ ≈ 43 (TripN(SiMe₃)₂).

4.2.6. Data for TripNH₃⁺Cl⁻·1.75 H₂O, 10·1.75 H₂O

The compound was formed during the purification of TripNH₂ **6** as described above, and the water content was estimated by integration of the ¹H NMR spectrum. ¹H NMR (499.9 MHz, CDCl₃, 298 K) δ = 1.24 (d, J_{HH} = 6.9 Hz, 6H, Ar-*p*-CH(CH₃)₂), 1.30 (d, J_{HH} = 6.5 Hz, 12H, Ar-*o*-CH(CH₃)₂), 1.68 (brs, ca. 3.5H, H₂O), 2.89 (sept, J_{HH} = 6.9 Hz, 1H, Ar-*p*-CH(CH₃)₂), 3.70 (sept, J_{HH} = 5.9 Hz, 2H, Ar-*o*-CH(CH₃)₂), 7.06 (s, 2H, Ar-*H*), 10.30 (brs, 3H, NH₃). ¹³C{¹H} NMR (125.7 MHz, CDCl₃, 298 K) δ = 24.1 (Ar-*p*-CH(CH₃)₂), 24.4 (Ar-*o*-CH(CH₃)₂), 28.6 (Ar-*o*-CH(CH₃)₂), 34.3 (Ar-*p*-CH(CH₃)₂), 122.4 (Ar-C), 123.5 (Ar-C), 142.7 (Ar-C), 149.5 (Ar-C).

4.3. Syntheses and Formation of Ter Compounds (14–17)

4.3.1. TerN(SiMe₃)Li **14**

TerLi(OEt₂) **11**(OEt₂) (9.5 mg, 16.9 μmol) was dissolved in C₆D₆ (0.5 mL) in a J. Young's NMR tube, after which THF (7.0 μL, 5.1 eq.) and Me₃SiN₃ (2.4 μL, 18 μmol, 1.07 eq.) were added. The sample was heated for 24 h at 60 °C, after which analysis by ¹H NMR spectroscopy showed complete consumption of TerLi·Et₂O **11**(OEt₂) and formation of TerN(SiMe₃)Li **14**. Further context is described in the main text. ¹H NMR (700.1 MHz, C₆D₆, 295 K) δ = -0.18 (s, 9H, Si(CH₃)₃), 1.24 (d, J_{HH} = 6.8 Hz, 12H, Trip-*o*-CH(CH₃)₂), 1.28 (d, J_{HH} = 7.0 Hz, 12H, Trip-*p*-CH(CH₃)₂), 1.40 (d, J_{HH} = 6.9 Hz, 12H, Trip-*o*-CH(CH₃)₂), 2.84 (sept, 2H, Trip-*p*-CH(CH₃)₂), 3.47 (m, 4H, Trip-*o*-CH(CH₃)₂), 6.87 (t, J_{HH} = 7.3 Hz, 1H, *p*-C₆H₃), 7.23 (d, J_{HH} = 7.3 Hz, 2H, *m*-C₆H₃), 7.24 (s, 4H, *m*-Trip). ⁷Li NMR (155.5 MHz, C₆D₆) δ = -0.81 (N(SiMe₃)Li). ¹³C{¹H} NMR (176.0 MHz, C₆D₆, 295 K) δ = 3.3 (Si(CH₃)₃), 23.8 (Trip-*o*-CH(CH₃)₂), 24.4 (Trip-*p*-CH(CH₃)₂), 26.4 (Trip-*o*-CH(CH₃)₂), 30.5 (Trip-*o*-CH(CH₃)₂), 34.7 (Trip-*p*-CH(CH₃)₂), 112.9 (Ar-C), 121.7 (Ar-C), 131.4 (Ar-C), 132.9 (Ar-C), 140.9 (Ar-C), 147.6 (Ar-C), 148.4 (Ar-C), 159.0 (Ar-C). ¹H-¹⁵N HMBS NMR (700.1/70.9 MHz, C₆D₆, 295 K) δ ≈ 115 (TerN(SiMe₃)Li).

4.3.2. Partial NMR Data for TerN₂N(SiMe₃)Li **15**

Compound TerN₂N(SiMe₃)Li **15** is formed as an intermediate during the reaction between TerLi(OEt₂) **11**(OEt₂) and Me₃SiN₃ in C₆D₆ with or without additional donor solvents. It was observed using ¹H NMR spectroscopy by tracking the apparent triplet at 6.98 ppm (*p*-C₆H₃), doublet at 7.12 ppm (*m*-C₆H₃) and a singlet at 0.03 ppm (Si(CH₃)₃). ¹H-¹⁵N HMBS NMR (700.1/70.9 MHz, C₆D₆, 295 K) δ ≈ 317 (TerN₂N(SiMe₃)Li).

4.3.3. Partial NMR Data for TerH

TerH is formed as a by-product during the reaction between TerLi(OEt₂) **11**(OEt₂) and Me₃SiN₃ in C₆D₆ with or without the addition of donor solvents. It was observed using ¹H NMR spectroscopy by tracking the singlet at 7.21 ppm (*m*-Trip).

4.3.4. Synthesis of TerN(SiMe₃)H **16**

A Schlenk flask was charged with TerI **12** (1.00 g, 1.64 mmol), *n*-hexane (ca. 25 mL) and Et₂O (ca. 10 mL). The reaction mixture was cooled to -50 °C using a cold bath and *n*BuLi (1.03 mL, 1.6 M solution in hexanes, ca. 1 eq.) was added dropwise. The reaction mixture was allowed to slowly warm to room temperature and stirred for an additional 2 h. All volatiles were removed in vacuo affording a white powder which was extensively dried for 1h, after which toluene (ca. 20 mL), THF (1.34 mL, 10 eq.) and Me₃SiN₃ (0.30 mL, 2.28 mmol, 1.4 eq.) were added. The resulting mixture was heated for 20 h to 60 °C, after which it was placed in an ice bath and methanol (10 mL) was added slowly over a period of 5 min, after which all volatiles were removed in vacuo. Dichloromethane (ca. 20 mL) and water (ca. 20 mL) were added, and organic layer was separated. Removal of volatiles in vacuo afforded crude product as a white solid, which was purified by recrystallisation from cold (room temperature to -40 °C) diethyl ether and afforded as two crops. Crystals suitable for X-ray crystallographic analysis were obtained upon storage of concentrated diethyl ether solution at 6 °C. Yield = 0.56 g (60%). ¹H NMR (700.1 MHz, C₆D₆, 295 K) δ = -0.34 (s, 9H,

Si(CH₃)₃, 1.16 (d, $J_{\text{HH}} = 6.8$ Hz, 12H, Trip-*o*-CH(CH₃)₂), 1.29 (d, $J_{\text{HH}} = 7.0$ Hz, 12H, Trip-*p*-CH(CH₃)₂), 1.38 (d, $J_{\text{HH}} = 6.9$ Hz, 12H, Trip-*o*-CH(CH₃)₂), 2.87 (sept, $J_{\text{HH}} = 6.9$ Hz, 2H, Trip-*p*-CH(CH₃)₂), 3.06 (sept, $J_{\text{HH}} = 6.8$ Hz, 4H, Trip-*o*-CH(CH₃)₂), 3.24 (s, 1H, N(SiMe₃)H), 6.92 (t, $J_{\text{HH}} = 7.5$ Hz, 1H, *p*-C₆H₃), 7.19 (d, $J_{\text{HH}} = 7.5$ Hz, 2H, *m*-C₆H₃), 7.23 (s, 4H, *m*-Trip). ¹³C{¹H} NMR (176.0 MHz, C₆D₆, 295 K) $\delta = 0.4$ (Si(CH₃)₃), 23.8 (Trip-*o*-CH(CH₃)₂), 24.4 (Trip-*p*-CH(CH₃)₂), 26.2 (Trip-*o*-CH(CH₃)₂), 30.9 (Trip-*o*-CH(CH₃)₂), 34.9 (Trip-*p*-CH(CH₃)₂), 119.3 (Ar-C), 121.6 (Ar-C), 131.3 (Ar-C), 131.4 (Ar-C), 135.7 (Ar-C), 144.9 (Ar-C), 148.0 (Ar-C), 149.0 (Ar-C). ¹H-¹⁵N HMBS NMR (700.1/70.9 MHz, C₆D₆, 295 K) $\delta \approx 67$ (TerN(SiMe₃)H).

4.3.5. Deprotection of TerN(SiMe₃)H **16**: Synthesis of TerNH₂ **17**

NMR scale experiments have shown that TerN(SiMe₃)H **16** could be deprotected with silica or by prolonged standing in wet CDCl₃ to obtain the corresponding aniline TerNH₂ **17**, a known compound [78]. On a large scale it is more convenient to deprotect **16** using aqueous HCl. TerN(SiMe₃)H **16** (120 mg, 0.20 mmol) was dissolved in diethyl ether (12 mL), and conc. aq. HCl (37%, 0.5 mL) was added dropwise, and the resulting solution was stirred at room temperature for 1 h, after which aqueous (saturated) Na₂CO₃ solution (20 mL) was added, and the resulting mixture was stirred for 30 min. The organic layer was separated, and the aqueous layer was extracted with dichloromethane (ca. 15 mL). The organic fractions were combined, and the solvent was removed in vacuo, affording solid TerNH₂ **17** which was isolated and dried under vacuum. (Note: an additional extraction step with dichloromethane may be required if insoluble material is present, e.g., NaHCO₃). Yield = 90 mg (86%). ¹H NMR (500.1 MHz, CDCl₃, 295 K) $\delta = 1.10$ (d, $J_{\text{HH}} = 6.9$ Hz, 12H, Trip-*o*-CH(CH₃)₂), 1.12 (d, $J_{\text{HH}} = 6.8$ Hz, 12H, Trip-*o*-CH(CH₃)₂), 1.30 (d, $J_{\text{HH}} = 6.9$ Hz, 12H, Trip-*p*-CH(CH₃)₂), 2.75 (sept, $J_{\text{HH}} = 6.8$ Hz, 4H, Trip-*o*-CH(CH₃)₂), 2.94 (sept, $J_{\text{HH}} = 6.9$ Hz, 2H, Trip-*p*-CH(CH₃)₂), 3.14 (brs, 2H, NH₂), 6.81 (t, $J_{\text{HH}} = 7.4$ Hz, 1H, *p*-C₆H₃), 6.96 (d, $J_{\text{HH}} = 7.4$ Hz, 2H, *m*-C₆H₃), 7.08 (s, 4H, *m*-Trip).

4.4. Syntheses of ^RTrip_{nacnac}H Compounds **18–20**

4.4.1. MeTrip_{nacnac}H **18**

A round bottom flask was charged with pentane-2,4-dione (1.07 mL, 10.42 mmol, 1.0 equiv), *para*-toluenesulfonic acid monohydrate, *p*TsOH·H₂O (2.18 g, 11.46 mmol, 1.10 eq.), TripNH₂ **6** (4.81 g, 21.9 mmol, 2.10 eq.) and toluene (90 mL), and equipped with a Dean-Stark trap and a reflux condenser. The flask was placed in an oil bath and the reaction mixture was heated under reflux for 24 h to remove the water. Subsequently, most of the solvent (ca. 85 mL) was distilled off via the Dean-Stark trap leaving a dark brown oily residue. The oil was taken up in saturated aqueous Na₂CO₃ solution (ca. 100 mL) and dichloromethane (ca. 100 mL) and stirred until two clear phases formed. The organic layer was separated, and all volatiles were reduced in vacuo giving a dark viscous oil. Addition of methanol (20 mL) results in almost immediate precipitation of MeTrip_{nacnac}H **18** as an off-white solid which is subsequently isolated by filtration and washed with cold methanol (ca. 20 mL). Concentrating the supernatant solution to ca. 10 mL and storing at −40 °C afforded additional colourless crystals of **6** that were suitable for X-ray crystallographic analysis. Yield = 4.00 g (76%). M.p. 158–161 °C. ¹H NMR (500.1 MHz, CDCl₃, 295 K) $\delta = 1.12$ (d, $J_{\text{HH}} = 6.9$ Hz, 12H, Ar-*o*-CH(CH₃)₂), 1.21 (d, $J_{\text{HH}} = 6.9$ Hz, 12H, Ar-*o*-CH(CH₃)₂), 1.25 (d, $J_{\text{HH}} = 6.9$ Hz, 12H, Ar-*p*-CH(CH₃)₂), 1.73 (s, 6H, NCCH₃), 2.87 (sept, $J_{\text{HH}} = 6.9$ Hz, 2H, Ar-*p*-CH(CH₃)₂), 3.09 (sept, $J_{\text{HH}} = 6.9$ Hz, 4H, Ar-*o*-CH(CH₃)₂), 4.85 (s, 1H, NC(CH₃)CH), 6.95 (s, 4H, Ar-*H*), 12.15 (s, 1H, NH). ¹H NMR (400.1 MHz, C₆D₆, 294 K) $\delta = 1.21$ (d, $J_{\text{HH}} = 6.9$ Hz, 12H, Ar-*o*-CH(CH₃)₂), 1.29 (d, $J_{\text{HH}} = 7.0$ Hz, 12H, Ar-*o*-CH(CH₃)₂), 1.30 (d, $J_{\text{HH}} = 6.9$ Hz, 12H, Ar-*p*-CH(CH₃)₂), 1.71 (s, 6H, NCCH₃), 2.88 (sept, $J_{\text{HH}} = 6.9$ Hz, 2H, Ar-*p*-CH(CH₃)₂), 3.35 (sept, $J_{\text{HH}} = 6.9$ Hz, 4H, Ar-*o*-CH(CH₃)₂), 4.90 (s, 1H, NC(CH₃)CH), 7.17 (s, 4H, Ar-*H*), 12.61 (s, 1H, NH). ¹³C{¹H} NMR (100.6 MHz, C₆D₆, 295 K): $\delta = 20.8$ (NCCH₃), 23.7 (Ar-*o*-CH(CH₃)₂), 24.6 (Ar-*o*-CH(CH₃)₂ or Ar-*p*-CH(CH₃)₂), 24.6 (Ar-*o*-CH(CH₃)₂ or Ar-*p*-CH(CH₃)₂), 28.8 (Ar-*o*-CH(CH₃)₂), 34.8 (Ar-*p*-CH(CH₃)₂), 94.1 (NC(CH₃)CH), 121.4 (Ar-C), 139.2 (Ar-C), 142.7 (Ar-C), 145.9 (Ar-C), 161.7 (NCCH₃).

4.4.2. ^{Et}Trip_{nacnac}H 19

A round bottom flask was charged with heptane-3,5-dione (1.45 mL, 1.37 g, 10.42 mmol), *para*-toluenesulfonic acid monohydrate, *p*TsOH·H₂O (2.24 g, 11.46 mmol, 1.10 eq.), TripNH₂ 6 (4.94 g, 21.93 mmol, 2.10 eq.) and xylene (mixture of isomers, 90 mL), and equipped with a Dean-Stark trap, a reflux condenser, and a nitrogen inlet with oil bubbler. The flask was placed in an oil bath and nitrogen gas was blown through the apparatus for a few minutes to displace most of the air. The reaction mixture was refluxed under a very slow nitrogen flow for 48 h to remove the water. Subsequently, the majority of the solvent (ca. 80 mL) was distilled off via the Dean-Stark trap leaving a dark brown oily residue. The oil was taken up in a saturated aqueous Na₂CO₃ solution (ca. 100 mL) and dichloromethane (ca. 100 mL) and stirred until two clear phases formed. The organic layer was separated, and all volatiles were reduced in vacuo giving a dark viscous oil that was dried under vacuum. Addition of methanol (30 mL) with prolonged sonication resulted in the precipitation of ^{Et}Trip_{nacnac}H 19 as an off-white solid which was subsequently isolated by filtration and washed with cold methanol (ca. 20 mL). Colourless crystals suitable for X-ray crystallographic analysis were obtained by redissolving 19 in boiling methanol and subsequent cooling to room temperature. Yield = 3.77 g (66%). M.p. 142–145 °C. ¹H NMR (500.1 MHz, CDCl₃, 295 K) δ = 1.08 (t, *J*_{HH} = 7.6 Hz, 6H, NCCH₂CH₃), 1.10 (d, *J*_{HH} = 6.8 Hz, 12H, Ar-*o*-CH(CH₃)₂), 1.19 (d, *J*_{HH} = 6.9 Hz, 12H, Ar-*o*-CH(CH₃)₂), 1.25 (d, *J*_{HH} = 6.9 Hz, 12H, Ar-*p*-CH(CH₃)₂), 2.05 (q, *J*_{HH} = 7.6 Hz, 4H, NCCH₂CH₃), 2.87 (sept, *J*_{HH} = 6.9 Hz, 2H, Ar-*p*-CH(CH₃)₂), 3.07 (sept, *J*_{HH} = 6.9 Hz, 4H, Ar-*o*-CH(CH₃)₂), 4.91 (s, 1H, NC(CH₂CH₃)CH), 6.94 (s, 4H, Ar-*H*), 12.14 (s, 1H, NH). ¹H NMR (499.9 MHz, C₆D₆, 298 K) 0.98 (t, *J*_{HH} = 7.6 Hz, 6H, NCCH₂CH₃), 1.22 (d, *J*_{HH} = 6.8 Hz, 12H, Ar-*o*-CH(CH₃)₂), 1.30 (d, *J*_{HH} = 6.9 Hz, 12H, Ar-*p*-CH(CH₃)₂), 1.30 (d, *J*_{HH} = 6.9 Hz, 12H, Ar-*o*-CH(CH₃)₂), 2.13 (q, *J*_{HH} = 7.6 Hz, 4H, NCCH₂CH₃), 2.88 (sept, *J*_{HH} = 6.9 Hz, 2H, Ar-*p*-CH(CH₃)₂), 3.38 (sept, *J*_{HH} = 6.9 Hz, 4H, Ar-*o*-CH(CH₃)₂), 5.09 (s, 1H, NC(CH₂CH₃)CH), 7.18 (s, 4H, Ar-*H*), 12.64 (s, 1H, NH). ¹³C{¹H} NMR (125.7 MHz, C₆D₆, 298 K): δ = 12.1 (NCCH₂CH₃), 23.6 (Ar-*o*-CH(CH₃)₂), 24.6 (Ar-*p*-CH(CH₃)₂), 25.0 (Ar-*o*-CH(CH₃)₂), 26.8 (NCCH₂CH₃), 28.7 (Ar-*o*-CH(CH₃)₂), 34.8 (Ar-*p*-CH(CH₃)₂), 89.1 (NC(CH₂CH₃)CH), 121.4 (Ar-C), 138.8 (Ar-C), 142.8 (Ar-C), 145.8 (Ar-C), 166.9 (NCCH₃).

4.4.3. ^{iPr}Trip_{nacnac}H 20

A Schlenk flask with reflux condenser and nitrogen inlet was charged with P₄O₁₀ (10.1 g, 35.6 mmol) and hexamethyldisiloxane (25.0 mL, 117.6 mmol), and the mixture was dissolved in dry dichloromethane (25 mL). The reaction mixture was heated to reflux for 2 h under a gentle flow of nitrogen before cooling to 20 °C. All volatiles were removed in vacuo, affording a colourless, viscous syrup of PPSE. 2,6-dimethylheptane-3,5-dione (1.80 mL, 1.64 g, 10.5 mmol) and TripNH₂ 6 (4.70 g, 21.42 mmol, 2.04 eq.) were added to the flask under a gentle flow of nitrogen. The reaction mixture was then slowly heated to 170 °C and stirred for 48 h at this temperature. The reaction mixture was then cooled to ca. 95 °C and an aqueous NaOH solution (8.0 g in 100 mL) was carefully (exothermic reaction!) and slowly added via the top of the reflux condenser with vigorous stirring. After cooling, the formed solid residue was extracted with dichloromethane (ca. 80 mL), the organic layer was separated off, and all volatiles were removed in vacuo. Addition of methanol (25 mL) resulted in almost immediate precipitation of ^{iPr}Trip_{nacnac}H 20 as an off-white solid which was subsequently isolated by filtration and washed with cold methanol (ca. 20 mL). Colourless crystals suitable for X-ray crystallographic analysis were obtained by storing an *n*-hexane solution of 20 at 6 °C for two months. Yield = 3.90 g (67%). M.p. 204–207 °C. ¹H NMR (500.1 MHz, CDCl₃, 295 K) δ = 1.08 (ad, 24H, Ar-*o*-CH(CH₃)₂ and NC(CH(CH₃)₂), 1.22 (d, *J*_{HH} = 6.9 Hz, 12H, Ar-*o*-CH(CH₃)₂), 1.25 (d, *J*_{HH} = 6.9 Hz, 12H, Ar-*p*-CH(CH₃)₂), 2.43 (sept, *J*_{HH} = 6.8 Hz, 2H, NC(CH(CH₃)₂)), 2.87 (sept, *J*_{HH} = 6.9 Hz, 2H, Ar-*p*-CH(CH₃)₂), 3.07 (sept, *J*_{HH} = 6.8 Hz, 4H, Ar-*o*-CH(CH₃)₂), 4.89 (s, 1H, NC(CH(CH₃)₂)CH), 6.93 (s, 4H, Ar-*H*), 11.76 (s, 1H, NH). ¹H NMR (499.9 MHz, C₆D₆, 298 K) δ = 1.05 (d, *J*_{HH} = 6.8 Hz, 12H, NC(CH(CH₃)₂)), 1.23 (d, *J*_{HH} = 6.8 Hz, 12H, Ar-*o*-CH(CH₃)₂), 1.29 (d, *J*_{HH} = 6.9 Hz, 12H, Ar-*p*-CH(CH₃)₂), 1.34 (d, *J*_{HH} = 6.9 Hz, 12H, Ar-*o*-CH(CH₃)₂), 2.60 (sept, *J*_{HH} = 6.8 Hz, 2H,

NC(CH(CH₃)₂), 2.86 (sept, $J_{\text{HH}} = 7.0$ Hz, 2H, Ar-*p*-CH(CH₃)₂), 3.39 (sept, $J_{\text{HH}} = 6.9$ Hz, 4H, Ar-*o*-CH(CH₃)₂), 5.12 (s, 1H, NC(CH(CH₃)₂)CH), 7.18 (s, 4H, Ar-*H*), 12.36 (s, 1H, NH). ¹³C{¹H} NMR (125.7 MHz, C₆D₆, 298 K): $\delta = 22.2$ (NC(CH(CH₃)₂)), 23.6 (Ar-*o*-CH(CH₃)₂), 24.6 (Ar-*p*-CH(CH₃)₂), 25.7 (Ar-*o*-CH(CH₃)₂), 28.4 (Ar-*o*-CH(CH₃)₂), 30.4 (NC(CH(CH₃)₂)), 34.7 (Ar-*p*-CH(CH₃)₂), 84.0 (NC(CH(CH₃)₂)CH), 121.5 (Ar-C), 138.4 (Ar-C), 142.9 (Ar-C), 145.6 (Ar-C), 171.8 (NC(CH(CH₃)₂)).

4.5. Synthesis of [(ⁱPr^{Trip}nacnac)MgH]₂ **21**

A J Youngs flask was charged with ⁱPr^{Trip}nacnacH **20** (1.00 g, 1.79 mmol) and toluene (ca. 20 mL). The resulting solution was cooled using an ice bath and Mg*n*Bu₂ (2.33 mL, 1.0 M solution in heptane, 1.30 eq.) was added. The solution was then briefly heated to 50 °C for ca. 30 min and then stirred at room temperature for 16 h. The resulting reaction mixture was reduced in vacuo, redissolved in *n*-hexane (ca. 20 mL), a very small quantity of an insoluble precipitate was filtered off, and phenylsilane (0.29 mL, 2.35 mmol, 1.32 eq.) was added. The resulting mixture was heated to 60 °C for 48 h producing a fine white precipitate of **21**, that was isolated by hot filtration, washed with *n*-hexane (ca. 10 mL) and dried under vacuum. Colourless crystals of **21** suitable for X-ray crystallographic analysis were obtained by cooling a saturated solution in benzene from 60 °C to room temperature. Yield = 0.43 g (41%). ¹H NMR (499.9 MHz, C₆D₆, 298 K) $\delta = 0.94$ (d, $J_{\text{HH}} = 6.7$ Hz, 24H, NCCH(CH₃)₂), 1.00 (brs, 24H, Ar-*o*-CH(CH₃)₂), 1.34 (d, $J_{\text{HH}} = 7.1$ Hz, 24H, Ar-*o*-CH(CH₃)₂), 1.34 (d, $J_{\text{HH}} = 7.0$ Hz, 24H, Ar-*p*-CH(CH₃)₂), 2.53 (sept, $J_{\text{HH}} = 6.8$ Hz, 4H, NCCH(CH₃)₂), 2.89 (sept, $J_{\text{HH}} = 7.1$ Hz, 4H, Ar-*p*-CH(CH₃)₂), 3.19 (brsept, 8H, Ar-*o*-CH(CH₃)₂), 3.96 (s, 2H, Mg-*H*), 4.88 (s, 2H, NC(CH(CH₃)₂)CH), 7.08 (s, 8H, Ar-*H*). ¹H NMR (499.9 MHz, C₆D₆, 353 K) $\delta = 0.99$ (ad, 48H, Ar-*o*-CH(CH₃)₂ and NCCH(CH₃)₂), 1.30 (d, $J_{\text{HH}} = 6.8$ Hz, 24H, Ar-*o*-CH(CH₃)₂), 1.33 (d, $J_{\text{HH}} = 6.9$ Hz, 24H, Ar-*p*-CH(CH₃)₂), 2.54 (sept, $J_{\text{HH}} = 6.6$ Hz, 4H, NCCH(CH₃)₂), 2.88 (sept, $J_{\text{HH}} = 7.0$ Hz, 4H, Ar-*p*-CH(CH₃)₂), 3.17 (sept, $J_{\text{HH}} = 6.9$ Hz, 8H, Ar-*o*-CH(CH₃)₂), 3.93 (s, 2H, Mg-*H*), 4.91 (s, 2H, NC(CH(CH₃)₂)CH), 7.05 (s, 8H, Ar-*H*). ¹³C{¹H} NMR (125.7 MHz, C₆D₆, 353 K): $\delta = 23.3$ (NC(CH(CH₃)₂) or Ar-*o*-CH(CH₃)₂), 24.2 (Ar-*o*-CH(CH₃)₂ or Ar-*p*-CH(CH₃)₂), 24.4 (Ar-*o*-CH(CH₃)₂ or Ar-*p*-CH(CH₃)₂), 26.3 (NC(CH(CH₃)₂) or Ar-*o*-CH(CH₃)₂), 28.1 (Ar-*o*-CH(CH₃)₂), 32.0 (NC(CH(CH₃)₂)), 34.5 (Ar-*p*-CH(CH₃)₂), 85.5 (NC(CH(CH₃)₂)CH), 121.9 (Ar-C), 142.5 (Ar-C), 143.2 (Ar-C), 144.8 (Ar-C), 179.9 (NC(CH(CH₃)₂)).

4.6. X-Ray Crystallographic Details

X-ray diffraction data for compounds **16**, **16**·C₆H₆, **18**·C₇H₈, **20**, **21** were collected using a Rigaku FR-X Ultrahigh Brilliance Microfocus RA generator/confocal optics with XtaLAB P200 diffractometer [Mo K α radiation ($\lambda = 0.71073$ Å)]. Diffraction data for compounds **9** and **19** were collected using a Rigaku MM-007HF High Brilliance RA generator/confocal optics with XtaLAB P100 or P200 diffractometers [Cu K α radiation ($\lambda = 1.54187$ Å)]. Data for all compounds analysed were collected and processed (including correction for Lorentz, polarization, and absorption) using CrysAlisPro. [107] Structures were solved by dual space (SHELXT) [108] or direct (SIR2011) [109] methods. All structures were refined by full-matrix least-squares against F^2 (SHELXL-2019/3) [110]. Non-hydrogen atoms were refined anisotropically, and hydrogen atoms were refined using a riding model except for those on nitrogen atoms in **16**, **16**·C₆H₆, **18**·C₇H₈, and **19**, which were located from the difference Fourier map and refined isotropically subject to a distance restraint. The hydride hydrogen atoms in **21** were also located from the difference Fourier map and refined isotropically without distance restraints. All calculations were performed using the Olex2 [111] interface. Selected crystallographic data are presented below. CCDC 2301678–2301684 contains the supplementary crystallographic data for this paper. These data can be obtained free of charge from The Cambridge Crystallographic Data Centre via www.ccdc.cam.ac.uk/structures.

Crystal data for TripN(SiMe₃)₂ **9**: CCDC 2301680, C₂₁H₄₁NSi, $M = 363.73$, colourless prism, $0.06 \times 0.05 \times 0.04$ mm³, orthorhombic, space group *Aea*2 (No. 41), $a = 37.6202(5)$,

$b = 12.11603(15)$, $c = 15.74019(18)$ Å, $V = 7174.49(16)$ Å³, $Z = 12$, $D_c = 1.010$ g cm⁻³, $F_{000} = 2424$, $\mu = 1.343$ mm⁻¹, $T = 173$ K, $2\theta_{\max} = 151.4^\circ$, 66,014 reflections collected, 7404 unique ($R_{\text{int}} = 0.0494$). Final $GoF = 1.020$, $R_1 = 0.0339$, $wR_2 = 0.0863$, R indices based on 7141 reflections with $I > 2\sigma(I)$ (refinement on F^2), 359 parameters, 22 restraints. The molecule crystallised with 1.5 molecules in the asymmetric unit. The 4-isopropyl group in the half molecule is disordered and was refined with two positions for each atom using geometry restraints.

Crystal data for TerN(SiMe₃)H **16**: CCDC 2301681, C₃₉H₅₉NSi, $M = 569.96$, colourless prism, $0.16 \times 0.11 \times 0.04$ mm³, monoclinic, space group $P2_1/c$ (No. 14), $a = 19.3572(3)$, $b = 9.47187(15)$, $c = 19.6361(3)$ Å, $\beta = 95.6547(14)^\circ$, $V = 3582.73(10)$ Å³, $Z = 4$, $D_c = 1.057$ g cm⁻³, $F_{000} = 1256$, $\mu = 0.091$ mm⁻¹, $T = 173$ K, $2\theta_{\max} = 58.8^\circ$, 75,801 reflections collected, 8820 unique ($R_{\text{int}} = 0.0310$). Final $GoF = 1.035$, $R_1 = 0.0413$, $wR_2 = 0.1035$, R indices based on 7244 reflections with $I > 2\sigma(I)$ (refinement on F^2), 410 parameters, 4 restraints. The molecule crystallised with a full molecule in the asymmetric unit. One 4-isopropyl group is disordered and was refined with two positions for the atoms of the outer methyl groups using geometry restraints.

Crystal data for TerN(SiMe₃)H·C₆H₆ **16**·C₆H₆: CCDC 2301683, C₄₅H₆₅NSi, $M = 648.07$, colourless plate, $0.07 \times 0.06 \times 0.02$ mm³, monoclinic, space group $P2_1/n$ (No. 14), $a = 9.1204(2)$, $b = 19.8896(4)$, $c = 22.6572(5)$ Å, $\beta = 92.2103(19)^\circ$, $V = 4106.97(15)$ Å³, $Z = 4$, $D_c = 1.048$ g cm⁻³, $F_{000} = 1424$, $\mu = 0.086$ mm⁻¹, $T = 125$ K, $2\theta_{\max} = 58.3^\circ$, 178,448 reflections collected, 10365 unique ($R_{\text{int}} = 0.0671$). Final $GoF = 1.017$, $R_1 = 0.0490$, $wR_2 = 0.1076$, R indices based on 7382 reflections with $I > 2\sigma(I)$ (refinement on F^2), 454 parameters, 7 restraints. The molecule crystallised with a full molecule and one benzene molecule in the asymmetric unit. One 2-isopropyl group is disordered and was refined with two positions for the atoms of one methyl group and the methine-H using geometry restraints.

Crystal data for Me^{Trip}nacnacH·C₇H₈ **18**·C₇H₈: CCDC 2301684, C₄₂H₆₂N₂, $M = 594.93$, colourless prism, $0.12 \times 0.04 \times 0.03$ mm³, orthorhombic, space group $Pbca$ (No. 61), $a = 17.3978(6)$, $b = 17.1598(6)$, $c = 24.9732(8)$ Å, $V = 7455.6(4)$ Å³, $Z = 8$, $D_c = 1.060$ g cm⁻³, $F_{000} = 2624$, $\mu = 0.060$ mm⁻¹, $T = 120$ K, $2\theta_{\max} = 58.6^\circ$, 160,281 reflections collected, 9438 unique ($R_{\text{int}} = 0.1475$). Final $GoF = 1.022$, $R_1 = 0.0952$, $wR_2 = 0.1760$, R indices based on 5281 reflections with $I > 2\sigma(I)$ (refinement on F^2), 416 parameters, 1 restraint. The compound crystallised with one full molecule plus one toluene molecule in the asymmetric unit.

Crystal data for Et^{Trip}nacnacH **19**: CCDC 2301678, C₃₇H₅₈N₂, $M = 530.85$, colourless plate, $0.12 \times 0.11 \times 0.01$ mm³, monoclinic, space group $P2_1/c$ (No. 14), $a = 9.2583(6)$, $b = 25.5248(15)$, $c = 15.1348(8)$ Å, $\beta = 99.624(6)^\circ$, $V = 3526.3(4)$ Å³, $Z = 4$, $D_c = 1.000$ g cm⁻³, $F_{000} = 1176$, $\mu = 0.421$ mm⁻¹, $T = 173$ K, $2\theta_{\max} = 141.3^\circ$, 30,594 reflections collected, 6182 unique ($R_{\text{int}} = 0.0831$). Final $GoF = 1.060$, $R_1 = 0.0547$, $wR_2 = 0.1336$, R indices based on 3814 reflections with $I > 2\sigma(I)$ (refinement on F^2), 390 parameters, 9 restraints. The compound crystallised with a full molecule in the asymmetric unit. One backbone ethyl group is disordered and was modelled and refined with two positions for each atom.

Crystal data for iPr^{Trip}nacnacH **20**: CCDC 2301679, C₃₉H₆₂N₂, $M = 558.90$, colourless prism, $0.12 \times 0.06 \times 0.04$ mm³, orthorhombic, space group $Ibca$ (No. 73), $a = 16.1089(8)$, $b = 16.8884(10)$, $c = 26.3413(18)$ Å, $V = 7166.2(7)$ Å³, $Z = 8$, $D_c = 1.036$ g cm⁻³, $F_{000} = 2480$, $\mu = 0.059$ mm⁻¹, $\lambda = 0.71073$ Å, $T = 125$ K, $2\theta_{\max} = 58.3^\circ$, 38,250 reflections collected, 4425 unique ($R_{\text{int}} = 0.0410$). Final $GoF = 1.032$, $R_1 = 0.0850$, $wR_2 = 0.1897$, R indices based on 2675 reflections with $I > 2\sigma(I)$ (refinement on F^2), 224 parameters, 34 restraints. The compound crystallised with half a molecule in the asymmetric unit. The 4-isopropyl group is disordered and was modelled with two positions for each atom using geometry restraints.

Crystal data for [(iPr^{Trip}nacnac)MgH]₂ **21**: CCDC 2301682, C₃₉H₆₂N₂Mg, $M = 1166.42$, colourless block, $0.09 \times 0.09 \times 0.03$ mm³, orthorhombic, space group $Pbcn$ (No. 60), $a = 16.0213(5)$, $b = 17.4646(5)$, $c = 25.6440(7)$ Å, $V = 7175.3(4)$ Å³, $Z = 4$, $D_c = 1.080$ g cm⁻³, $F_{000} = 2576$, $\mu = 0.077$ mm⁻¹, $T = 125$ K, $2\theta_{\max} = 58.2^\circ$, 77,501 reflections collected, 8645 unique ($R_{\text{int}} = 0.0521$). Final $GoF = 1.031$, $R_1 = 0.0484$, $wR_2 = 0.1125$, R indices based

on 6107 reflections with $I > 2\sigma(I)$ (refinement on F^2), 399 parameters, 0 restraints. This compound crystallised with half a molecule in the asymmetric unit.

Supplementary Materials: The following supporting information can be downloaded at: <https://www.mdpi.com/article/10.3390/molecules28227569/s1>; Table S1: In-situ NMR scale study of reaction between $\text{TerLi}(\text{OEt}_2)$ $11(\text{OEt}_2)$ and Me_3SiN_3 ; IR spectrum (Figure S1), NMR spectroscopy (Figure S2–S38), Buried volume information, Table S2: Buried volume for $[(\text{R}^n\text{Ar}^n\text{acnac})\text{MgH}]_2$ complexes for the four quadrants and in total and Figures S39–S40.

Author Contributions: N.D. performed most experiments and compound characterisations, guided the main body of work, wrote the experimental section, and contributed to the results and discussion. M.G. and C.B. carried out experiments and characterisation. A.P.M. and D.B.C. conducted the X-ray crystallographic analyses. A.S. conceived and supervised the project and wrote the main section of the manuscript with input from all authors. All authors have read and agreed to the published version of the manuscript.

Funding: We are grateful to the EPSRC DTG (EP/T518062/1, EP/R513337/1), the School of Chemistry and the University of St Andrews for support.

Institutional Review Board Statement: Not applicable.

Informed Consent Statement: Not applicable.

Data Availability Statement: X-ray crystallographic data are available via the CCDC; please see the X-ray Section 4.5. The research data (NMR spectroscopy) supporting this publication can be accessed at <https://doi.org/10.17630/419a7764-7072-412a-b008-115c696fd9cd>.

Conflicts of Interest: The authors declare no conflict of interest.

References

1. Tsai, Y.-C. The chemistry of univalent metal β -diketimines. *Coord. Chem. Rev.* **2012**, *256*, 722–758. [[CrossRef](#)]
2. Bourget-Merle, L.; Lappert, M.F.; Severn, J.R. The chemistry of β -diketiminatometal complexes. *Chem. Rev.* **2002**, *102*, 3031–3065. [[CrossRef](#)] [[PubMed](#)]
3. Jones, C. Bulky guanidines for the stabilization of low oxidation state metallacycles. *Coord. Chem. Rev.* **2010**, *254*, 1273–1289. [[CrossRef](#)]
4. Kays, D.L. Extremely bulky amide ligands in main group chemistry. *Chem. Soc. Rev.* **2016**, *45*, 1004–1018. [[CrossRef](#)]
5. Cao, C.-S.; Shi, Y.; Xu, H.; Zhao, B. Metal–metal bonded compounds with uncommon low oxidation state. *Coord. Chem. Rev.* **2018**, *365*, 122–144. [[CrossRef](#)]
6. Noor, A. Coordination Chemistry of Bulky Aminopyridines with Main Group and Transition Metals. *Top. Curr. Chem.* **2021**, *379*, 6. [[CrossRef](#)] [[PubMed](#)]
7. Power, P.P. Main-group elements as transition metals. *Nature* **2010**, *463*, 171–177. [[CrossRef](#)]
8. Weetman, C.; Inoue, S. The road travelled: After main-group elements as transition metals. *ChemCatChem* **2018**, *10*, 4213–4228. [[CrossRef](#)]
9. Weetman, C. Main Group Multiple Bonds for Bond Activations and Catalysis. *Chem. Eur. J.* **2021**, *27*, 1941–1954. [[CrossRef](#)]
10. Forster, H.; Vögtle, F. Steric Interactions in Organic Chemistry: Spatial Requirements of Substituents. *Angew. Chem. Int. Ed. Engl.* **1977**, *16*, 429–441. [[CrossRef](#)]
11. Poater, A.; Cosenza, B.; Correa, A.; Giudice, S.; Ragone, F.; Scarano, V.; Cavallo, L. SambVca: A Web Application for the Calculation of the Buried Volume of *N*-Heterocyclic Carbene Ligands. *Eur. J. Inorg. Chem.* **2009**, *2009*, 1759–1766. [[CrossRef](#)]
12. Wagner, J.P.; Schreiner, P.R. London Dispersion in Molecular Chemistry—Reconsidering Steric Effects. *Angew. Chem. Int. Ed.* **2015**, *54*, 12274–12296. [[CrossRef](#)] [[PubMed](#)]
13. Liptrot, D.J.; Power, P.P. London dispersion forces in sterically crowded inorganic and organometallic molecules. *Nat. Rev. Chem.* **2017**, *1*, 0004. [[CrossRef](#)]
14. Mears, K.L.; Power, P.P. Beyond Steric Crowding: Dispersion Energy Donor Effects in Large Hydrocarbon Ligands. *Acc. Chem. Res.* **2022**, *55*, 1337–1348. [[CrossRef](#)]
15. Lalrempuia, R.; Kefalidis, C.E.; Bonyhady, S.J.; Schwarze, B.; Maron, L.; Stasch, A.; Jones, C. Activation of CO by Hydrogenated Magnesium(I) Dimers: Sterically Controlled Formation of Ethenediolate and Cyclopropanetriolate Complexes. *J. Am. Chem. Soc.* **2015**, *137*, 8944–8947. [[CrossRef](#)]
16. Mukherjee, D.; Okuda, J. Molecular Magnesium Hydrides. *Angew. Chem. Int. Ed.* **2018**, *57*, 1458–1473. [[CrossRef](#)]
17. Green, S.P.; Jones, C.; Stasch, A. Stable Magnesium(I) Compounds with Mg–Mg Bonds. *Science* **2007**, *318*, 1754–1757. [[CrossRef](#)]
18. Rösch, B.; Gentner, T.X.; Eysel, J.; Langer, J.; Elsen, H.; Harder, S. Strongly reducing magnesium(0) complexes. *Nature* **2021**, *592*, 717–721. [[CrossRef](#)]

19. Jones, C. Dimeric magnesium(I) β -diketiminates: A new class of quasi-universal reducing agent. *Nat. Rev. Chem.* **2017**, *1*, 0059. [[CrossRef](#)]
20. Queen, J.D.; Lehmann, A.; Fettingner, J.C.; Tuononen, H.M.; Power, P.P. The Monomeric Alane-diyl: AlAr^iPr^8 ($\text{Ar}^i\text{Pr}^8 = \text{C}_6\text{H}_2-2,6-(\text{C}_6\text{H}_2-2,4,6\text{Pr}^i_3)_2-3,5-\text{Pr}^i_2$): An Organoaluminum(I) Compound with a One-Coordinate Aluminum Atom. *J. Am. Chem. Soc.* **2020**, *142*, 20554–20559. [[CrossRef](#)]
21. Rit, A.; Campos, J.; Niu, H.; Aldridge, S. A stable heavier group 14 analogue of vinylidene. *Nat. Chem.* **2016**, *8*, 1022–1026. [[CrossRef](#)] [[PubMed](#)]
22. Liu, L.; Ruiz, D.A.; Munz, D.; Bertrand, G. A Singlet Phosphinidene Stable at Room Temperature. *Chem* **2016**, *1*, 147–153. [[CrossRef](#)]
23. Wu, M.; Li, H.; Chen, W.; Wang, D.; He, Y.; Xu, L.; Ye, S.; Tan, G. A triplet stibinidene. *Chem* **2023**, *9*, 1–12. [[CrossRef](#)]
24. Pang, Y.; Nöthling, N.; Leutzsch, M.; Kang, L.; Bill, E.; van Gastel, M.; Reijerse, E.; Goddard, R.; Wagner, L.; SantaLucia, D.; et al. Synthesis and isolation of a triplet bismuthinidene with a quenched magnetic response. *Science* **2023**, *380*, 1043–1048. [[CrossRef](#)] [[PubMed](#)]
25. Pratley, C.; Fenner, S.; Murphy, J.A. Nitrogen-Centered Radicals in Functionalization of sp^2 Systems: Generation, Reactivity, and Applications in Synthesis. *Chem. Rev.* **2022**, *122*, 8181–8260. [[CrossRef](#)]
26. Romanazzi, G.; Petrelli, V.; Fiore, A.M.; Mastroianni, P.; Dell’Anna, M.M. Metal-based Heterogeneous Catalysts for One-Pot Synthesis of Secondary Anilines from Nitroarenes and Aldehydes. *Molecules* **2021**, *26*, 1120. [[CrossRef](#)]
27. Saha, B.; De, S.; Dutta, S. Recent Advancements of Replacing Existing Aniline Production Process with Environmentally Friendly One-Pot Process: An Overview. *Crit. Rev. Environ. Sci. Techn.* **2013**, *43*, 84–120. [[CrossRef](#)]
28. Kienle, M.; Dubbaka, S.R.; Brade, K.; Knochel, P. Modern Amination Reactions. *Eur. J. Org. Chem.* **2007**, *2007*, 4166–4176. [[CrossRef](#)]
29. Cenini, S.; Gallo, E.; Caselli, A.; Ragaini, F.; Fantauzzi, S.; Piangiolino, C. Coordination chemistry of organic azides and amination reactions catalyzed by transition metal complexes. *Coord. Chem. Rev.* **2006**, *250*, 1234–1253. [[CrossRef](#)]
30. Intrieri, D.; Zardi, P.; Caselli, A.; Gallo, E. Organic azides: “Energetic reagents” for the intermolecular amination of C–H bonds. *Chem. Commun.* **2014**, *50*, 11440–11453. [[CrossRef](#)]
31. Corpet, M.; Gosmini, C. Recent Advances in Electrophilic Amination Reactions Electrophilic Amination Reactions. *Synthesis* **2014**, *46*, 2258–2271. [[CrossRef](#)]
32. Starkov, P.; Jamison, T.F.; Marek, I. Electrophilic Amination: The Case of Nitrenoids. *Chem. Eur. J.* **2015**, *21*, 5278–5300. [[CrossRef](#)]
33. Zhou, Z.; Kürti, L. Electrophilic Amination: An Update. *Synlett* **2019**, *30*, 1525–1535. [[CrossRef](#)]
34. O’Neil, L.G.; Bower, J.F. Electrophilic Aminating Agents in Total Synthesis. *Angew. Chem. Int. Ed.* **2021**, *60*, 25640–25666. [[CrossRef](#)] [[PubMed](#)]
35. Meiries, S.; Le Duc, G.; Chartoire, A.; Collado, A.; Speck, K.; Arachchige, K.S.A.; Slawin, A.M.Z.; Nolan, S.P. Large yet Flexible N-Heterocyclic Carbene Ligands for Palladium Catalysis. *Chem. Eur. J.* **2013**, *19*, 17358–17368. [[CrossRef](#)] [[PubMed](#)]
36. Savka, R.; Plenio, H. Metal Complexes of Very Bulky N,N' -Diarylimidazolylidene N-Heterocyclic Carbene (NHC) Ligands with 2,4,6-Cycloalkyl Substituents. *Eur. J. Inorg. Chem.* **2014**, *2014*, 6246–6253. [[CrossRef](#)]
37. Steele, B.R.; Georgakopoulos, S.; Micha-Screttas, M.; Screttas, C.G. Synthesis of New Sterically Hindered Anilines. *Eur. J. Org. Chem.* **2007**, *2007*, 3091–3094. [[CrossRef](#)]
38. Oleinik, I.I.; Oleinik, I.V.; Abdrakhmanov, I.B.; Ivanchev, S.S.; Tolstikov, G.A. Design of arylimine postmetallocene catalytic systems for olefin polymerization: I. Synthesis of substituted 2-cycloalkyl- and 2,6-dicycloalkylanilines. *Russ. J. Gen. Chem.* **2004**, *74*, 1423–1427. [[CrossRef](#)]
39. Atwater, B.; Chandrasoma, N.; Mitchell, D.; Rodriguez, M.J.; Pompeo, M.; Froeze, R.D.J.; Organ, M.G. The Selective Cross-Coupling of Secondary Alkyl Zinc Reagents to Five-Membered-Ring Heterocycles Using Pd-PEPPSI-IHep^{Cl}. *Angew. Chem. Int. Ed.* **2015**, *54*, 9502–9506. [[CrossRef](#)]
40. Bartlett, R.A.; Dias, H.V.R.; Power, P.P. Isolation and X-ray crystal structures of the organolithium etherate complexes, $[\text{Li}(\text{Et}_2\text{O})_2(\text{CPh}_3)]$ and $[\{\text{Li}(\text{Et}_2\text{O})(2,4,6-(\text{CHMe}_2)_3\text{C}_6\text{H}_2)\}_2]$. *J. Organomet. Chem.* **1988**, *341*, 1–9. [[CrossRef](#)]
41. Ruhlandt-Senge, K.; Ellison, J.J.; Wehmschulte, R.J.; Pauer, F.; Power, P.P. Isolation and Structural Characterization of Unsolvated Lithium Aryls. *J. Am. Chem. Soc.* **1993**, *115*, 11353–11357. [[CrossRef](#)]
42. Reich, H.J. Role of Organolithium Aggregates and Mixed Aggregates in Organolithium Mechanisms. *Chem. Rev.* **2013**, *113*, 7130–7178. [[CrossRef](#)] [[PubMed](#)]
43. Bailey, W.F.; Patricia, J.J. The Mechanism Of The Lithium–Halogen Interchange Reaction: A Review Of The Literature. *J. Organomet. Chem.* **1988**, *352*, 1–46. [[CrossRef](#)]
44. Applequist, D.E.; O’Brien, D.F. Equilibria in Halogen–Lithium Interconversions. *J. Am. Chem. Soc.* **1962**, *85*, 743–748. [[CrossRef](#)]
45. Jedlicka, B.; Crabtree, R.H.; Siegbahn, P.E.M. Origin of Solvent Acceleration in Organolithium Metal–Halogen Exchange Reactions. *Organometallics* **1997**, *16*, 6021–6023. [[CrossRef](#)]
46. Tai, O.; Hopson, R.; Williard, P.G. Aggregation and Solvation of n-Butyllithium. *Org. Lett.* **2017**, *19*, 3966–3969. [[CrossRef](#)]
47. Bailey, W.F.; Luderer, M.R.; Jordan, K.P. Effect of Solvent on the Lithium–Bromine Exchange of Aryl Bromides: Reactions of n-Butyllithium and tert-Butyllithium with 1-Bromo-4-tert-butylbenzene at 0 °C. *J. Org. Chem.* **2006**, *71*, 2825–2828. [[CrossRef](#)]
48. Gorecka-Kobylnska, J.; Schlosser, M. Relative Basicities of ortho-, meta-, and para-Substituted Aryllithiums. *J. Org. Chem.* **2009**, *74*, 222–229. [[CrossRef](#)]

49. Shi, L.; Chu, Y.; Knochel, P.; Mayr, H. Kinetics of Bromine-Magnesium Exchange Reactions in Substituted Bromobenzenes. *J. Org. Chem.* **2009**, *74*, 2760–2764. [[CrossRef](#)]
50. Merrill, R.E.; Negishi, E.-I. Tetrahydrofuran-Promoted Aryl-Alkyl Coupling Involving Organolithium Reagents. *J. Org. Chem.* **1974**, *39*, 3452–3453. [[CrossRef](#)]
51. Maercker, A. Ether Cleavage with Organo-Alkali-Metal Compounds and Alkali Metals. *Angew. Chem. Int. Ed. Engl.* **1987**, *26*, 972–989. [[CrossRef](#)]
52. McGarrity, J.F.; Ogle, C.A.; Brich, Z.; Loosli, H.-R. A Rapid-Injection NMR Study of the Reactivity of Butyllithium Aggregates in Tetrahydrofuran. *J. Am. Chem. Soc.* **1985**, *107*, 1810–1815. [[CrossRef](#)]
53. Bräse, S.; Gil, C.; Knepper, K.; Zimmermann, V. Organic Azides: An Exploding Diversity of a Unique Class of Compounds. *Angew. Chem. Int. Ed.* **2005**, *44*, 5188–5240. [[CrossRef](#)] [[PubMed](#)]
54. Chiba, S. Application of Organic Azides for the Synthesis of Nitrogen-Containing Molecules. *Synlett* **2012**, *1*, 21–44. [[CrossRef](#)]
55. Xie, S.; Sundhoro, M.; Houk, K.N.; Yan, M. Electrophilic Azides for Materials Synthesis and Chemical Biology. *Acc. Chem. Res.* **2020**, *53*, 937–948. [[CrossRef](#)] [[PubMed](#)]
56. Zhu, L.; Kinjo, R. Reactions of main group compounds with azides forming organic nitrogen-containing species. *Chem. Soc. Rev.* **2023**, *52*, 5563–5606. [[CrossRef](#)] [[PubMed](#)]
57. Kimball, D.B.; Haley, M.M. Triazenes: A Versatile Tool in Organic Synthesis. *Angew. Chem. Int. Ed.* **2002**, *41*, 3338–3351. [[CrossRef](#)]
58. Hauber, S.-O.; Lissner, F.; Deacon, G.B.; Niemeyer, M. Stabilization of Aryl—Calcium, —Strontium, and —Barium Compounds by Designed Steric and π -Bonding Encapsulation. *Angew. Chem. Int. Ed.* **2005**, *44*, 5871–5875. [[CrossRef](#)]
59. McKay, A.I.; Cole, M.L. Structural diversity in a homologous series of donor free alkali metal complexes bearing a sterically demanding triazenide. *Dalton Trans.* **2019**, *48*, 2948–2952. [[CrossRef](#)]
60. Wiberg, N.; Nerudu, B. Darstellung, Eigenschaften und Struktur einiger Silylazide. *Chem. Ber.* **1966**, *99*, 740–749. [[CrossRef](#)]
61. Wiberg, N.; Joo, W.-C. Zur Umsetzung von Silylaziden mit Grignard-Verbindungen. *J. Organomet. Chem.* **1970**, *22*, 333–340. [[CrossRef](#)]
62. Wiberg, N.; Joo, W.-C.; Olbert, P. Zum Mechanismus der Umsetzung von Silylaziden mit Grignard-Verbindungen (Zur Frage der Reaktivität von Grignard-Verbindungen). *J. Organomet. Chem.* **1970**, *22*, 341–348. [[CrossRef](#)]
63. Wiberg, N.; Joo, W.-C. Zum Mechanismus der Thermolyse von Silylazid-Grignard-Addukten (Zur Frage der Reaktivität Der N-Diazoniumgruppe). *J. Organomet. Chem.* **1970**, *22*, 349–356. [[CrossRef](#)]
64. Wiberg, N.; Pracht, H.J. Darstellung und Eigenschaften einiger Silyltriazene. *Chem. Ber.* **1972**, *105*, 1377–1387. [[CrossRef](#)]
65. Wiberg, N.; Pracht, H.J. Zur 1.3-Wandertendenz von Silylgruppen in Silyltriazenen. *Chem. Ber.* **1972**, *105*, 1388–1391. [[CrossRef](#)]
66. Wiberg, N.; Pracht, H.J. Zur cis-trans-Isomerie von Silyltriazenen. *Chem. Ber.* **1972**, *105*, 1392–1398. [[CrossRef](#)]
67. Wiberg, N.; Pracht, H.J. Zur gehinderten Rotation in Silyltriazenen. *Chem. Ber.* **1972**, *105*, 1399–1402. [[CrossRef](#)]
68. Nishiyama, K.; Tanaka, N. Synthesis and reactions of trimethylsilylmethyl azide. *J. Chem. Soc. Chem. Commun.* **1983**, 1322–1323. [[CrossRef](#)]
69. Sieburth, S.M.; Somers, J.J.; O'Hare, H.K. α -Alkyl- α -aminosilanes. 1. Metalation and alkylation between silicon and nitrogen. *Tetrahedron* **1996**, *52*, 5669–5682. [[CrossRef](#)]
70. Kulyabin, P.S.; Izmer, V.V.; Goryunov, G.P.; Sharikov, M.I.; Kononovich, D.S.; Uborsky, D.V.; Canich, J.-A.M.; Voskoboynikov, A.Z. Multisubstituted C₂-symmetric ansa-metallocenes bearing nitrogen heterocycles: Influence of substituents on catalytic properties in propylene polymerization at higher temperatures. *Dalton Trans.* **2021**, *50*, 6170–6180. [[CrossRef](#)]
71. Trost, B.M.; Pearson, W.H. Azidomethyl Phenyl Sulfide. A Synthon for NH₂⁺. *J. Am. Chem. Soc.* **1981**, *103*, 2483–2485. [[CrossRef](#)]
72. Trost, B.M.; Pearson, W.H. Sulfur activation of azides toward addition of organometallics. Amination of aliphatic carbanions. *J. Am. Chem. Soc.* **1983**, *105*, 1054–1056. [[CrossRef](#)]
73. Trost, B.M.; Pearson, W.H. A synthesis of the naphthalene core of streptovaricin D via A synthon of NH₂⁺. *Tetrahedron Lett.* **1983**, *24*, 269–272. [[CrossRef](#)]
74. Krasovskiy, A.; Straub, B.F.; Knochel, P. Highly efficient Reagents for Br/Mg exchange. *Angew. Chem. Int. Ed.* **2005**, *45*, 159–162. [[CrossRef](#)] [[PubMed](#)]
75. Mori, S.; Aoyama, T.; Shioiri, T. New Methods and Reagents in Organic Synthesis. 60. A New Synthesis of Aromatic and Heteroaromatic Amines Using Diphenyl Phosphorazidate (DPPA). *Chem. Pharm. Bull.* **1986**, *34*, 1524–1530. [[CrossRef](#)]
76. Hassner, A.; Munger, P.; Belinka, B.A., Jr. A novel amination of aromatic and heteroaromatic compounds. *Tetrahedron Lett.* **1982**, *23*, 699–702. [[CrossRef](#)]
77. Kabalka, G.W.; Li, G. Synthesis of aromatic amines using allyl azide. *Tetrahedron Lett.* **1997**, *38*, 5777–5778. [[CrossRef](#)]
78. Twamley, B.; Hwang, C.-S.; Hardman, N.J.; Power, P.P. Sterically encumbered terphenyl substituted primary pnictanes ArEH₂ and their metallated derivatives ArE(H)Li (Ar = -C₆H₃-2,6-Trip₂; Trip = 2,4,6-triisopropylphenyl; E = N, P, As, Sb). *J. Organomet. Chem.* **2000**, *609*, 152–160. [[CrossRef](#)]
79. Wright, R.J.; Steiner, J.; Beaini, S.; Power, P.P. Synthesis of the sterically encumbering terphenyl silyl and alkyl amines HN(R)Ar^{Mes2} (R = Me and SiMe₃), their lithium derivatives LiN(R)Ar^{Mes2}, and the tertiary amine Me₂NAr^{Mes2}. *Inorg. Chim. Acta* **2006**, *359*, 1939–1946. [[CrossRef](#)]
80. Gavenonis, J.; Schüwer, N.; Tilley, T.D.; Boynton, J.N.; Power, P.P. 2,6-Dimesitylaniline (H₂NC₆H₃-2,6-Mes₂) and 2,6-bis(2,4,6-triisopropylphenyl)aniline (H₂NC₆H₃-2,6-Trip₂). In *Inorganic Syntheses*; Power, P.P., Ed.; John Wiley & Sons: Hoboken, NJ, USA, 2018; Volume 37, pp. 98–105.

81. Grubert, L.; Jacobi, D.; Buck, K.; Abraham, W.; Mügge, C.; Krause, E. Pseudorotaxanes and Rotaxanes Incorporating Cycloheptatrienyl Stations—Synthesis and Co-Conformation. *Eur. J. Org. Chem.* **2001**, *2001*, 3921–3932. [CrossRef]
82. Liu, J.-Y.; Zheng, Y.; Li, Y.-G.; Pan, L.; Li, Y.-S.; Hu, N.-H. Fe(II) and Co(II) pyridinebisimine complexes bearing different substituents on ortho- and para-position of imines: Synthesis, characterization and behavior of ethylene polymerization. *J. Organomet. Chem.* **2005**, *690*, 1233–1239. [CrossRef]
83. Sadique, A.R.; Gregory, E.A.; Brennessel, W.W.; Holland, P.L. Mechanistic Insight into N=N Cleavage by a Low-Coordinate Iron(II) Hydride Complex. *J. Am. Chem. Soc.* **2007**, *129*, 8112–8121. [CrossRef] [PubMed]
84. Hering-Junghans, C.; Schulz, A.; Thomas, M.; Villinger, A. Synthesis of mono-, di-, and triaminobismuthanes and observation of C–C coupling of aromatic systems with bismuth(III) chloride. *Dalton Trans.* **2016**, *45*, 6053–6059. [CrossRef] [PubMed]
85. Wang, T.; Hoffmann, M.; Dreuw, A.; Hasagić, E.; Hu, C.; Stein, P.M.; Witzel, S.; Shi, H.; Yang, Y.; Rudolph, M.; et al. A metal-free direct arene C–H amination. *Adv. Synth. Cat.* **2021**, *363*, 2783–2795. [CrossRef]
86. Axenrod, T.; Mangiaracina, P.; Pregosin, P.S. A ¹³C- and ¹⁵N-NMR. Study of Some 1-Aryl-3, 3-dimethyl Triazene Derivatives. *Helv. Chim. Act.* **1976**, *59*, 1655–1660. [CrossRef]
87. Ide, S.; Iwasawa, K.; Yoshino, A.; Yoshida, T.; Takahashi, K. NMR study of the lithium salts of aniline derivatives. *Magn. Reson. Chem.* **1987**, *25*, 675–679. [CrossRef]
88. Merz, K.; Bieda, R. In situ Crystallization of N(SiMe₃)₃ and As(SiMe₃)₃: Trigonal planar or pyramidal coordination of the central atoms? *Z. Kristallogr.* **2014**, *229*, 635–638. [CrossRef]
89. Barnett, B.R.; Mokhtarzadeh, C.C.; Figueroa, J.S.; Lummis, P.; Wang, S.; Queen, J.D. m-Terphenyl IODO and Lithium Reagents Featuring 2,6-bis-(2,6-diisopropylphenyl) Substitution Patterns and an m-Terphenyl Lithium Etherate Featuring the 2,6-bis-(2,4,6-TRIIISOPROPYLPHENYL) Substitution Pattern. In *Inorganic Syntheses*; Power, P.P., Ed.; John Wiley & Sons: Hoboken, NJ, USA, 2018; Volume 37, pp. 89–98.
90. Moore, D.R.; Cheng, M.; Lobkovsky, E.B.; Coates, G.W. Mechanism of the Alternating Copolymerization of Epoxides and CO₂ Using β-Diiminate Zinc Catalysts: Evidence for a Bimetallic Epoxide Enchainment. *J. Am. Chem. Soc.* **2003**, *125*, 11911–11924. [CrossRef]
91. Arrowsmith, M.; Maitland, B.; Kociok-Köhn, G.; Stasch, A.; Jones, C.; Hill, M.S. Mononuclear Three-Coordinate Magnesium Complexes of a Highly Sterically Encumbered β-Diketiminato Ligand. *Inorg. Chem.* **2014**, *53*, 10543–10552. [CrossRef]
92. Ma, M.-T.; Shen, X.C.; Yu, Z.J.; Yao, W.W.; Du, L.T.; Xu, L.S.B. β-Diketiminato Magnesium Complexes: Syntheses, Crystal Structure and Catalytic Hydrosilylation. *Chin. J. Inorg. Chem.* **2016**, *32*, 1857–1866. Available online: <http://www.ccsublishing.org.cn/article/doi/10.11862/CJIC.2016.232> (accessed on 7 November 2023).
93. Gentner, T.X.; Rösch, B.; Ballmann, G.; Langer, J.; Elsen, H.; Harder, S. Low Valent Magnesium Chemistry with a Super Bulky β-Diketiminato Ligand. *Angew. Chem. Int. Ed.* **2019**, *58*, 607–611. [CrossRef]
94. Bakhoda, A.G.; Jiang, Q.; Badiel, Y.M.; Bertke, J.A.; Cundari, T.R.; Warren, T.H. Copper-Catalyzed C(sp³)-H Amidation: Sterically Driven Primary and Secondary C-H Site-Selectivity. *Angew. Chem. Int. Ed.* **2019**, *58*, 3421–3425. [CrossRef] [PubMed]
95. Yuvaraj, K.; Douair, I.; Jones, D.D.L.; Maron, L.; Jones, C. Sterically controlled reductive oligomerisations of CO by activated magnesium(I) compounds: Deltate vs. ethenediolate formation. *Chem. Sci.* **2020**, *11*, 3516–3522. [CrossRef] [PubMed]
96. Rösch, B.; Gentner, T.X.; Eyslein, J.; Friedrich, A.; Langer, J.; Harder, S. Mg–Mg bond polarization induced by a superbulky β-diketiminato ligand. *Chem. Commun.* **2020**, *56*, 11402–11405. [CrossRef]
97. Jones, D.D.L.; Watts, S.; Jones, C. Synthesis and Characterization of Super Bulky β-Diketiminato Group 1 Metal Complexes. *Inorganics* **2021**, *9*, 72. [CrossRef]
98. Mindiola, D.J.; Holland, P.L.; Warren, T.H. Complexes of Bulky β-Diketiminato Ligands. In *Inorganic Syntheses*; Rauchfuss, T.B., Ed.; John Wiley & Sons: Hoboken, NJ, USA, 2010; Volume 35, pp. 1–55.
99. Burnett, S.; Bourne, C.; Slawin, A.M.Z.; van Mourik, T.; Stasch, A. Umpolung of an Aliphatic Ketone to a Magnesium Ketone-1, 2-diide Complex with Vicinal Dianionic Charge. *Angew. Chem. Int. Ed.* **2022**, *61*, e202204472. [CrossRef]
100. López, S.E.; Restrepo, J.; Salazar, J. Polyphosphoric acid trimethylsilyl ester: A useful reagent for organic synthesis. *J. Chem. Res.* **2007**, *2007*, 497–502. [CrossRef]
101. Yamamoto, K.; Watanabe, H. Composition of “Polyphosphoric Acid Trimethylsilyl Ester (PPSE)” and Its Use as a Condensation Reagent. *Chem. Lett.* **1982**, *11*, 1225–1228. [CrossRef]
102. Roy, M.M.D.; Omanaña, A.A.; Wilson, A.S.S.; Hill, M.S.; Aldridge, S.; Rivard, E. Molecular Main Group Metal Hydrides. *Chem. Rev.* **2021**, *121*, 12784–12965. Available online: <https://pubs.acs.org/doi/epdf/10.1021/acs.chemrev.1c00278> (accessed on 7 November 2023). [CrossRef]
103. Green, S.P.; Jones, C.; Stasch, A. Stable Adducts of a Dimeric Magnesium(I) Compound. *Angew. Chem. Int. Ed.* **2008**, *47*, 9079–9083. [CrossRef]
104. Bonyhady, S.J.; Jones, C.; Nembenna, S.; Stasch, A.; Edwards, A.J.; McIntyre, G.J. β-Diketiminato-Stabilized Magnesium(I) Dimers and Magnesium(II) Hydride Complexes: Synthesis, Characterization, Adduct Formation, and Reactivity Studies. *Chem. Eur. J.* **2010**, *16*, 938–955. [CrossRef] [PubMed]
105. Treitler, D.S.; Leung, S. How Dangerous Is Too Dangerous? A Perspective on Azide Chemistry. *J. Org. Chem.* **2022**, *87*, 11293–11295. [CrossRef] [PubMed]
106. Conrow, R.E.; Dean, W.D. Diazidomethane Explosion. *Org. Proc. Res. Dev.* **2008**, *12*, 1285–1286. [CrossRef]
107. *CrysAlisPro v1.171.42.94a Rigaku Oxford Diffraction*; Rigaku Corporation: Tokyo, Japan, 2023.

108. Sheldrick, G.M. SHELXT—Integrated space-group and crystal structure determination. 2. *Acta Crystallogr. Sect. A Found. Adv.* **2015**, *71*, 3–8. [[CrossRef](#)] [[PubMed](#)]
109. Burla, M.C.; Caliandro, R.; Camalli, M.; Carrozzini, B.; Cascarano, G.L.; Giacovazzo, C.; Mallamo, M.; Mazzone, A.; Polidori, G.; Spagna, R. SIR2011: A new package for crystal structure determination and refinement. *J. Appl. Crystallogr.* **2012**, *45*, 357–361. [[CrossRef](#)]
110. Sheldrick, G.M. Crystal structure refinement with SHELXL. *Acta Crystallogr. Sect. C Struct. Chem.* **2015**, *71*, 3–8. [[CrossRef](#)]
111. Dolomanov, O.V.; Bourhis, L.J.; Gildea, R.J.; Howard, J.A.K.; Puschmann, H. OLEX2: A complete structure solution, refinement and analysis program. *J. Appl. Crystallogr.* **2009**, *42*, 339–341. [[CrossRef](#)]

Disclaimer/Publisher’s Note: The statements, opinions and data contained in all publications are solely those of the individual author(s) and contributor(s) and not of MDPI and/or the editor(s). MDPI and/or the editor(s) disclaim responsibility for any injury to people or property resulting from any ideas, methods, instructions or products referred to in the content.